Neuroscience and Biobehavioral Reviews 112 (2020) 452–471

Contents lists available at ScienceDirect

Neuroscience and Biobehavioral Reviews

journal homepage: www.elsevier.com/locate/neubiorev

Neural circuits of idiopathic Normal Pressure Hydrocephalus: A perspective review of brain connectivity and symptoms meta-analysis

Alessandra Griffa[a,b,*], Dimitri Van De Ville[b,c], François R. Herrmann[d], Gilles Allali[a,e,f]

[a] Department of Clinical Neurosciences, Division of Neurology, Geneva University Hospitals and Faculty of Medicine, University of Geneva, Geneva, Switzerland
[b] Institute of Bioengineering, Center of Neuroprosthetics, Ecole Polytechnique Fédérale De Lausanne (EPFL), Lausanne, Switzerland
[c] Department of Radiology and Medical Informatics, University of Geneva, Geneva, Switzerland
[d] Department of Rehabilitation and Geriatrics, Geneva University Hospitals and University of Geneva, Geneva, Switzerland
[e] Faculty of Medicine, University of Geneva, Geneva, Switzerland
[f] Department of Neurology, Division of Cognitive & Motor Aging, Albert Einstein College of Medicine, Yeshiva University, Bronx, NY, USA

ARTICLE INFO

Keywords:
Idiopathic normal pressure hydrocephalus
Reversible dementia
Brain connectivity
Locomotion
Functional MRI
Diffusion MRI
EEG
Brain network
Meta-analysis
Activation likelihood estimation
Connectome

ABSTRACT

Idiopathic normal pressure hydrocephalus (iNPH) is a prevalent reversible neurological disorder characterized by impaired locomotion, cognition and urinary control with ventriculomegaly. Symptoms can be relieved with cerebrospinal fluid drainage, which makes iNPH the leading cause of reversible dementia. Because of a limited understanding of pathophysiological mechanisms, unspecific symptoms and the high prevalence of comorbidity (i.e. Alzheimer's disease), iNPH is largely underdiagnosed. For these reasons, there is an urgent need for developing noninvasive quantitative biomarkers for iNPH diagnosis and prognosis. Structural and functional changes of brain circuits in relation to symptoms and treatment response are expected to deliver major advances in this direction. We review structural and functional brain connectivity findings in iNPH and complement those findings with iNPH symptom meta-analyses in healthy populations. Our goal is to reinforce our conceptualization of iNPH as to brain network mechanisms and foster the development of new hypotheses for future research and treatment options.

1. Introduction

Idiopathic Normal Pressure Hydrocephalus (iNPH) is a progressive and debilitating neurological disorder characterized by gait impairments, cognitive decline and urinary incontinence with ventricles enlargement at brain imaging (Gallia et al., 2006; Relkin et al., 2005; Williams and Malm, 2016). The disorder was first described in 1965 by Salómon Hakim, who reported three patients with symptomatic ventriculomegaly but normal cerebrospinal fluid (CSF) pressure, and unexpected symptom reversal after CSF drainage (Hakim and Adams, 1965; Wallenstein and McKhann, 2010). Since this initial description, iNPH has received growing attention by the neurology and neuroimaging communities, representing the leading cause of reversible dementia. According to a large population-based Swedish study, the prevalence of iNPH is around 6% of adults older than 80 years (Halperin et al., 2015; Jaraj et al., 2014). However, iNPH clinical presentation is unspecific and imaging features (i.e. ventriculomegaly) can be confused with subcortical brain atrophy, leading to a possible underdiagnosis. At present, no quantitative clinical or neuroimaging marker with diagnostic or prognostic value is available for iNPH, which urges a more detailed characterization of the pathophysiological mechanisms and structural and functional brain-circuit changes that underly symptoms' appearance and reversal.

According to the international guidelines, the diagnosis of iNPH relies on the combination of brain imaging and clinical features (Marmarou et al., 2005; Relkin et al., 2005; Williams and Malm, 2016). These include evidence of communicating ventriculomegaly, normal-range CSF opening pressure (5–18 mmHg), and presence of at least one out of the three iNPH symptoms. Radiological signs of iNPH are a positive Evan's index (a ventricular frontal horn ratio larger than 0.3 (Evans, 1942)); narrow sulci at the median brain surface; enlarged Sylvian fissures and ventricular temporal horns; reduced callosal angle; presence of periventricular hyperintensities. These features have been summarized in a radiological score that correlates with symptoms and can be used for iNPH assessment in clinical practice (Kockum et al., 2018). Despite these instruments, the diagnosis of iNPH remains

* Corresponding author at: Campus Biotech, H4 3 232.080 (H4 building), Chemin des Mines 9, Case postale 60, CH-1211, Geneva, Switzerland.
E-mail addresses: alessandra.griffa@epfl.ch (A. Griffa), dimitri.vandeville@epfl.ch (D. Van De Ville), Francois.Herrmann@unige.ch (F.R. Herrmann), gilles.allali@hcuge.ch (G. Allali).

https://doi.org/10.1016/j.neubiorev.2020.02.023
Received 6 November 2019; Received in revised form 9 January 2020; Accepted 17 February 2020
Available online 20 February 2020

challenging: iNPH symptoms are not specific and can be found in other neurological disorders, such as Parkinson's disease and progressive supranuclear palsy (Allali et al., 2016; Jeppsson et al., 2019; Magdalinou et al., 2013). Moreover, iNPH is often associated with comorbid neurological (e.g., Alzheimer's disease) and non-neurological (e.g., arthritis) conditions (Allali et al., 2018a,b; Malm et al., 2013a; Pyykkö et al., 2018). A task force appointed by the International Society for Hydrocephalus and Cerebrospinal Fluid Disorders concludes that comorbidity in iNPH may explain the variation in prognosis and post-operative outcomes among different hydrocephalus centers (Malm et al., 2013b).

The treatment of iNPH is invasive and relies on the implant of a ventricular or lumbar shunt. Early treatment tends to improve the outcome, which emphasizes the need for early diagnostic markers (Andrén et al., 2014). Clinical improvement after shunt surgery has been registered in as low as 33 %, but up to 84 % of cases, depending on the outcome assessment procedure (Kubo et al., 2008), the timing of assessment (months, one year or later), and the selection criteria for treatment candidates through pre-surgical prognostic tests (Giordan et al., 2018; Klassen and Ahlskog, 2011; Klinge et al., 2012; Pomeraniec et al., 2016; Shaw et al., 2016; Toma et al., 2013). The latter include CSF infusion tests, quantifying the pre-surgical absorptive capacity of the CSF system, and CSF drainage tests, evaluating short-term clinical changes after an isolated CSF withdrawal with lumbar puncture (tap test) or multi-day drainage. iNPH prognostic tests have reasonably high sensitivity (73–100 % depending on the study), but very low specificity (16–42 %) and, therefore, poor accuracy in predicting surgery response (Halperin et al., 2015; Isaacs et al., 2019; Luikku et al., 2016; Marmarou et al., 2005; Wikkelsø et al., 2013).

iNPH has been associated with multiple reversible and irreversible neurobiological mechanisms (Keong et al., 2016; Williams and Malm, 2016). Diffusion tensor imaging (DTI) and finite element simulations indicate mechanical compression and stretching of periventricular brain tissues (Hoza et al., 2015; Kim et al., 2015; Peña et al., 2002; Siasios et al., 2016), accompanied by small blood-vessels damages causing local ischemia and microbleeds. Arterial spin labeling (ASL) and positron emission tomography (PET) show reduced cerebral blood flow in subcortical, frontal and temporal lobes, and decreased subcortical metabolism (Keong et al., 2016; Tarnaris et al., 2009). Alterations of CSF production and turnover can also contribute to iNPH pathophysiology: Altered CSF dynamics are associated with the development of interstitial edema and poor clearance of neurotoxic compounds, leading to the accumulation of redox products and pathogenic macromolecules (such as beta amyloid and tau peptides) in brain tissues. Altogether, these mechanical, vascular and CSF-flow mechanisms are likely to induce both reversible and long-term grey and white matter changes, affecting brain functions and ultimately producing clinical symptoms. Nonetheless, the structural and functional consequences of these pathophysiological mechanisms on large-scale brain circuits remain largely unexplored.

Due to convergent but unspecific diagnostic criteria, the presence of neurological mimics, the high prevalence of comorbidities, the absence of reliable predictors of shunt response, and a limited understanding of pathophysiological mechanisms, iNPH is currently largely underdiagnosed and undertreated (Halperin et al., 2015; Jaraj et al., 2014). It is estimated that only 8% of subjects affected by iNPH receive disease-specific surgical treatment (Halperin et al., 2015). The development of quantitative and accurate markers for iNPH diagnosis and prognosis is therefore much needed. Such biomarkers should be non-invasive (likely based on neuroimaging techniques), clearly relate to ongoing neurobiological processes, and link structural brain changes to functional circuits and symptoms.

With the continuous development of cutting-edge imaging (including resting-state and task-based functional MRI (fMRI), source-level magnetoencephalography (MEG), electroencephalography (EEG), transcranial magnetic stimulation (TMS) and diffusion weighted imaging (DWI)), image processing and data analysis techniques, the last decades have seen an upsurge of neuroimaging studies investigating large-scale brain circuits in normal and pathological conditions including aging and dementia (Fornito et al., 2015; Griffa et al., 2013; Pievani et al., 2014; Preti et al., 2017; Stam, 2014). In iNPH, symptoms cannot be ascribed to isolated neural regions but result from the impaired interaction between multiple brain regions, calling for a circuit-level/brain-network perspective of the disorder. The holistic conceptualization of the brain as a network of interconnected regions can also favor the development of new hypotheses on the emergence, development and clinical manifestation of brain disorders. For example, brain connectivity studies have offered important insights into Alzheimer's and Parkinson's diseases, two of the most frequent comorbidities of iNPH, by recognizing patterns of pathogenic spread through synaptically coupled brain networks (Greicius and Kimmel, 2012; Raj et al., 2012; Zeighami et al., 2015). These patterns are able to predict disease evolution and prognosis, and they offer a link between local neurobiological processes and large-scale effects. Considering the current lack of iNPH markers, brain connectivity approaches appear to be an important instrument for the investigation of this complex disorder, particularly in relation to functional plasticity mechanisms and symptom reversibility. These analyses should build up on our current understanding of iNPH affected brain circuits, which we discuss in this article.

In this review, we follow two complementary approaches to pinpoint the brain circuits involved in iNPH pathophysiology and disentangle their role with respect to symptoms. We will first provide a timely and thorough survey of studies investigating brain connectivity features in iNPH, both from a structural and a functional perspective, including MRI (DWI, fMRI, structural MRI), EEG and TMS analyses. We will present findings in relation to key questions of iNPH, such as iNPH (differential) diagnosis and association between neuroimaging measures, symptoms and treatment response. Second, we will perform a set of meta-analyses of task-based functional studies of healthy populations investigating the neural substrates of locomotion, micturition and cognition (limited to executive function), which represent the three clinical domains affected in iNPH. We will study the union and intersection of the identified brain circuits to pinpoint possible "hubs of vulnerability" in iNPH. Establishing the brain circuits impaired in iNPH, in relation to those associated with iNPH symptoms in healthy populations, reinforces our conceptualization of iNPH and foster the development of new hypotheses for future research and treatment options.

2. Methods

2.1. Literature search and selection of studies

An extensive literature search of the PubMed database and articles screening were performed in October 2019, according to the PRISMA (Preferred Reporting Items for Systematic reviews and Meta-Analyses) guidelines (Moher et al., 2009) (Fig. 1). The papers' selection was performed by two authors (AG, GA) in parallel; no disagreement was present between the two authors. Three distinct queries were submitted: (i) a combination of the terms 'connectivity' or 'network', and any combination of the terms 'idiopathic', 'normal', 'pressure', 'hydrocephalus' (which returned 29 articles); (ii) a combination of a functional connectivity assessment technique ('functional MRI', 'fMRI', 'electroencephalography', 'EEG', 'magnetoencephalography', 'MEG', 'functional near infrared spectroscopy', 'fNIRS', 'transcranial magnetic stimulation', 'TMS', 'positron emission tomography', 'PET'), and any combination of the terms 'idiopathic', 'normal', 'pressure', 'hydrocephalus' (which returned 303 articles); (iii) a combination of a structural connectivity assessment technique ('diffusion tensor imaging', 'DTI', 'diffusion weighted imaging', 'DWI', 'diffusion MRI', 'tractography', 'covariance'), and any combination of the terms 'idiopathic',

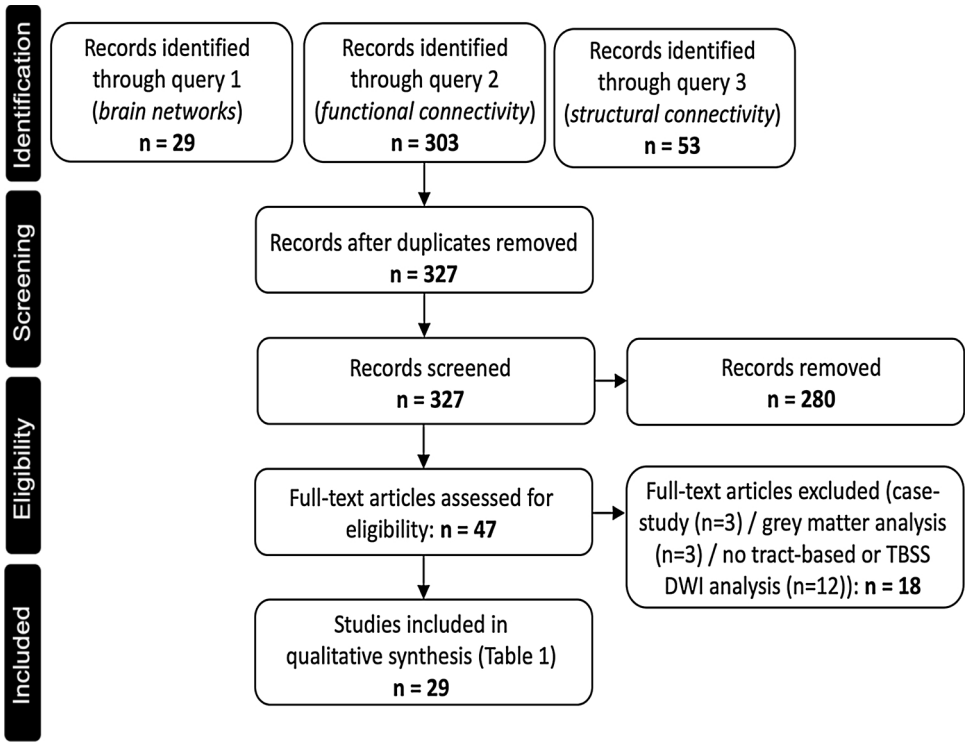

Fig. 1. PRISMA flow chart (Moher et al., 2009) illustrating the articles' selection process for the literature review. This includes PubMed entries' identification, screening, eligibility assessment and final selection. The screening process was based on articles' title and abstract screening: articles not written in English language, brief letters or commentaries, case reports, pediatric hydrocephalus studies, non-human hydrocephalus studies, clinical guidelines, reviews and articles including morphometric, volumetric, CSF dynamics, cerebral perfusion, brain tissue viscoelasticity, brain tissue compliance, glucose metabolism, amyloid or tau imaging, magnetic resonance spectroscopy or glymphatic imaging measures only (i.e., no brain connectivity measures) were excluded. Full-length articles surviving the screening process were assessed for eligibility: case reports, articles reporting DWI white matter properties based on regions of interest -with no tractography or TBSS connectivity analysis-, and articles investigating tissue properties of grey matter regions only (such as thalamic nuclei or hippocampi) were excluded.

'normal', 'pressure', 'hydrocephalus' (which returned 53 articles). The outputs of the PubMed searches were manually screened to exclude duplicates, single-patient case reports, studies investigating secondary or obstructive NPH or pediatric hydrocephalus cases, reviews, and articles not written in English language. Moreover, only studies satisfying the following criteria were included: (i) report *original neuroimaging data* of subjects with probable, possible, definite or not otherwise specified iNPH, and (ii) report at least one measure of *brain connectivity or functional activation*, such as statistical relationships between functional signals, power spectral analysis of functional signals, TMS measures, inter-subject covariance of cortical morphological features, brain network features, and/or tract-specific measures of white matter microstructure (including tract-based spatial statistics (TBSS) analyses (Smith et al., 2006)). Region-of-interest and voxel-based analyses with no tract-specific assessment were not included since no direct brain connectivity information could be extracted. For a review of iNPH findings in region-of-interest studies and other neuroimaging approaches (e.g., volumetry, metabolism, white matter lesions, CSF and cerebral blood flow assessment) we refer to (Hoza et al., 2015; Keong et al., 2016; Siasios et al., 2016; Tarnaris et al., 2009).

2.2. ALE meta-analyses

To identify candidate brain circuits vulnerable to iNPH pathophysiology, three activation likelihood estimation (ALE) meta-analyses of *task-contrast functional studies in healthy populations* were performed. An ALE meta-analysis determines the statistical convergence of the activation foci reported by different studies (Eickhoff et al., 2009; Turkeltaub et al., 2002). Here, we considered studies investigating brain activations related to the iNPH symptom triad: *locomotion*, *micturition* and *cognition*.

To be included in each meta-analysis, a study had to meet the following criteria: (i) contain task-contrast functional analyses (fMRI, PET, SPECT) of healthy subjects only, and (ii) report positive activation loci coordinates in MNI or Talairach space (Talairach coordinates were converted to MNI space (Lancaster et al., 2007)). Study search was performed in the BrainMap database (http://brainmap.org) using Sleuth v3.0.3 (Fox et al., 2005; Fox and Lancaster, 2002), and including additional works identified by the authors or cited in recent related meta-analyses (Boyne et al., 2018; Harvie et al., 2019), without the intention of being exhaustive with respect to literature. We searched for the following task-contrasts: (i) actual or imagined locomotion (e.g., walking, gait initiation, etc.) contrasted with a non-locomotion task (e.g., imagined standing or lying); (ii) micturition control (e.g., bladder filling or voiding, withholding urine, pelvic floor contraction, etc.) contrasted with a control condition (e.g., pelvic floor relaxation or rest); (iii) executive function quantified with the Eriksen flanker or modified flanker test (Eriksen and Schultz, 1979). This test requires the subject to focus on a central visual stimulus (typically, an arrow) and to promptly react to it while ignoring simultaneous and distracting, congruent or incongruent stimuli (e.g., lateral arrows pointing in the same or different directions than the central one) (Diamond, 2013; Eriksen and Schultz, 1979). The flanker is a relatively pure test that taps top-down regulation of attention, a core process of executive control (Diamond, 2013; Jurado and Rosselli, 2007). Executive function is specifically affected in iNPH and impairments appear early in the course of the disease (Picascia et al., 2016; Saito et al., 2011).

Once a set of MNI coordinates was collected for each one of the three functional domains (locomotion, micturition and cognition), the convergence of activation foci across experiments was assessed with random-effect ALE meta-analyses using GingerALE v3.0.2 (Turkeltaub et al., 2012). Results from non-independent contrasts (i.e., contrasts evaluated on the same or overlapping groups of subjects) were grouped in the same experiment before running the ALE algorithm. Briefly, the ALE algorithm converts each activation focus into a three-dimensional Gaussian probability distribution whose aperture depends on the sample size of the experiment (Eickhoff et al., 2009). The probability distributions of all the foci reported in a single experiment are then combined into a single Modeled Activation map representing the maximum probability across foci. Finally, an ALE probabilistic map is computed over all the experiments by taking the union probability of the Modeled Activation maps. An ALE map expresses the voxel-wise convergence of activation foci across experiments, and its statistical significance is assessed non-parametrically with a permutation

procedure that assigns a p-value to each voxel. The p-value maps obtained from the locomotion, micturition and cognition meta-analyses were thresholded at $p < .001$ (uncorrected), and clusters smaller than 100 mm^3 were discarded.

Finally, the union and intersection of the three ALE maps were estimated to identify candidate brain circuits and 'hot spots' vulnerable to iNPH pathophysiology. The union map was computed as the union probability of the thresholded ALE maps, i.e., $p_i = 1 - \prod_{k=1}^{3}(1 - p_i^k)$, with p_i union probability of voxel i across the three functional domains, and p_i^k ALE value of voxel i in the thresholded ALE map k. The intersection maps were computed by taking the minimum statistic across ALE maps, which identifies voxels where convergent activation was present for all the three (or two) functional domains. The centroids of the intersection maps were anatomically labelled using the Talairach Daemon (Lancaster et al., 2000) and associated to anatomical and behavioral keywords using the Neurosynth database (Yarkoni et al., 2011).

3. Results

3.1. Part 1 - Structural and functional connectivity findings in iNPH

From the PubMed literature search and manual screening of the studies, 29 articles were included in this review of brain connectivity and functional activity findings in iNPH (Table 1, Fig. 1). 6 studies investigated measures of functional connectivity in the brain as derived from EEG (n = 1), fMRI (n = 2) or TMS (n = 3), 5 studies analyzed EEG cortical power spectral or current source density features, and 1 study investigated fMRI cortical activation during task execution. 16 articles dealt with white-matter connectivity measures derived from DWI, and 1 article described grey matter volume covariance networks. The iNPH cohorts included in the studies were fairly homogeneous in terms of age (mean and approximate minimum-maximum age across studies: 75.4 (41–85) years for functional studies; 75.4 (65–86) years for structural studies). Studies tended to include a slightly higher proportion of males than females (56.7 % (44–69 %) for functional studies; 54.3 % (30–70 %) for structural studies).

We organize the review of the selected literature into thematic sections, with a particular attention to neural circuits and brain networks.

3.1.1. Methods to assess brain connectivity

The term *brain connectivity* refers to the presence of a structural or functional relationship between two neural regions, ranging from grey matter voxels to larger cortical, subcortical or cerebellar areas. A structural connection defines the presence of a white matter bundle connecting two grey matter regions and can be assessed using DWI and tractography algorithms. Different DWI sequences exist. While they all probe the directions of water molecule diffusion in brain tissues -which are parallel to nervous bundles in the white matter-, they differ in terms of MRI acquisition parameters, diffusion model assumptions, and types of diffusion measures that can be computed (Hagmann et al., 2006; Tournier et al., 2011). The most common DWI sequence used in this review is Diffusion Tensor Imaging (DTI) (Table 1). DTI assumes that the local diffusion process is Gaussian and models it with a diffusion tensor (Bihan et al., 2001). Parameters describing the elongation of the tensor (fractional anisotropy (FA)), the amount of water molecule displacement along the main diffusion direction (axial diffusivity (D_{axial})) or in the plane perpendicular to the main diffusion direction (radial diffusivity (D_{radial})), and the mean amount of diffusion (mean diffusivity (MD)) have been loosely related to white matter microstructural properties in healthy and pathological conditions, including Alzheimer's disease, Parkinson's disease and iNPH (Alexander et al., 2007; Beaulieu, 2002; Hattori et al., 2011; Siasios et al., 2016). For example, an increased D_{radial} can be interpreted as myelination loss, edema, or increased axonal diameter, whereas D_{axial} has been associated with axonal injury, axonal density and fiber orientation spread (Jones et al., 2013). DTI measures are non-specific and fail to model crossing-fiber areas but are highly reproducible across studies. More advanced DWI techniques disentangle the contribution of tissue microstructural properties to DWI scalars but require longer MRI acquisitions. Among the methods adopted in this review, Diffusion Kurtosis Imaging (DKI) (Fieremans et al., 2011; Jensen and Helpern, 2010), Free Water Imaging (FWI) (Pasternak et al., 2009), and Neurite Orientation Dispersion and Density Imaging (NODDI) (Zhang et al., 2012) model the local diffusion process with non-Gaussian and/or multi-factor equations that distinguish different microstructural environments (intra-cellular, extra-cellular and CSF compartments). The scalar measures derived from these models, such as the fiber orientation dispersion index (related to the local coherence of fiber directions), diffusion kurtosis (associated with microstructural complexity), free water volume fraction (an indicator of voxel-wise CSF contamination or interstitial edema), axonal water fraction (related to the axonal density) provide a more accurate and interpretable description of the white matter microstructure.

The voxel-wise diffusion directions estimated from DWI data are fed to tractography algorithms to reconstruct the white matter bundles connecting brain region pairs (Behrens et al., 2007). Once a bundle has been delineated, the strength of the structural connection can be quantified with the average DWI scalar measure computed along the tract (Tract-Specific Analysis (TSA)). Other MRI contrasts can be used as well. For example, a study quantifies the connectivity strength as the average magnetization transfer ratio along the tract, which is proportional to the myelin content (Jurcoane et al., 2014; Schmierer et al., 2004). While TSA relies on prior hypotheses on tracts of interest, hypothesis-free connectivity analyses investigate the whole-brain connectivity architecture (or *connectome* (Hagmann, 2005; Sporns et al., 2005)), or the connectivity strength along the main white matter tracts' skeleton (Tract-Based Spatial Statistics (TBSS) (Smith et al., 2006)).

Functional connectivity is defined as statistical interdependencies between brain signals (e.g., fMRI, EEG time series) recorded at two different grey matter locations (Friston, 1994) and represents patterns of synchronization (or communication) in the brain (van den Heuvel and Hulshoff Pol, 2010). Functional connectivity is impaired in multiple neuropsychiatric conditions, including neurodegenerative disorders (Greicius, 2008; Stam et al., 2007). Methods quantifying functional connectivity rely on pair-wise amplitude or phase relationships between signals (such as the linear correlation between two time series) or multivariate techniques. Among the latter, Independent Component Analysis (ICA) decomposes a whole-brain functional recording into a set of spatially independent maps with coherent temporal activity. Each brain map and its associated time series represent a behaviorally meaningful resting state network whose activation can be studied at the single-subject level using dual regression (Calhoun and Adali, 2006; Nickerson et al., 2017). A particular technique probing functional connectivity is TMS, a non-invasive method that stimulates excitatory synapses in the brain and can elicit muscular contractions through corticospinal tract and callosal signaling (Pascual-Leone et al., 2000; Rothwell et al., 2009). By applying different combinations of magnetic pulses, TMS is used to characterize intracortical connectivity (e.g., quantified by intracortical inhibition indexes in conditioning tests) and corticospinal tract excitability (e.g., assessing the resting motor threshold -the minimum stimulus intensity to elicit a motor response- or the central motor conduction time).

Besides functional connectivity, some of the reviewed articles investigated functional properties of individual brain regions (Aoki et al., 2015, 2013; Ikeda et al., 2015; Seo et al., 2014) (Table 1). EEG data are classically analyzed by decomposing the signals into functionally distinct frequency bands (such as delta (0.5 – 4 Hz), theta (4 – 8 Hz), alpha (8 – 13 Hz), beta (13 – 30 Hz), gamma (40 – 48 Hz)) and computing the relative power content, its temporal variability (normalized power variance), or the current source density in each frequency band (Hari

Table 1
Brain connectivity findings in idiopathic Normal Pressure Hydrocephalus.

Study	Sample	Demographics of iNPH patients	Imaging	Brain connectivity or activity measure(s)	Main research question(s) and regions of interest	Key positive findings	Key negative findings
Functional connectivity and activity studies							
(Aoki et al., 2019)	58 iNPH	78.0 ± 6.0 y 57 % M	EEG	ICA dual-regression scores	- iNPH pre/post-TT (5 predefined RSNs)	• pre/post-TT alpha connectivity changes in **occipital**, **superior parietal**, **HPC**regions correlate with pre/post-TT changes of gait parameters	• no pre/post-TT changes of RSNs activity
(Aoki et al., 2015)	18 iNPH	75.0 ± 6.1 y 61 % M	EEG	band power content, NPV (electrode level)	- iNPH shunt responders/ non-responders (whole brain)	• ↑baseline β NPV in **right frontal**, **temporal**, **occipital areas** in responders compared to non-responders	• no differences of power spectral measures between responders and non-responders
(Aoki et al., 2013)	24 iNPH 52 NC	76.5 ± 5.3 y 54 % M	EEG	band power content, NPV (electrode level)	- iNPH pre/post-TT - iNPH shunt (or TT) responders/non-responders (whole brain)	• ↓ϑ, ↑γ power in **frontal/DLPC** channels after TT in non-responders only • pre/post-TT changes of NPV are specific to responders (↓α NPV in **medial prefrontal cortex**) and non-responders (normalization of α NPV in **DLPC**) • pre/post-TT α NPV decrease in **frontal areas** correlates with improvement of gait and cognitive scores when pooling responders and non-responders	• no pre/post-TT power changes in responders • no correlations between pre/post-TT power and functional score differences
(Chistyakov et al., 2012)	23 p-iNPH 8 NC 19 NC_{young} 9 patients (peripheral nerve disorders)	75.0 ± 7.8 y 52 % M	TMS	RMT, SICI	- iNPH-NC - iNPH pre/post-shunt (**CST**; **left motor area**)	• ↓ baseline RMT, SICI in iNPH compared to NC, NCyoung, other patients • ↑RMT, SICI after shunt in iNPH with gait improvements (assessment performed 1 month after surgery) • SICI post-shunt increase correlates with gait improvements	• baseline RMT, SICI did not predict post-shunt clinical improvement
(Ikeda et al., 2015)	25 s-iNPH	77.2 ± 5.1 y 56 % M	EEG	CSD (source level)	-iNPH shunt responders/ non-responders (whole brain, pre- and post-TT)	• ↑CSD in **frontal and temporal areas**in shunt responders compared to non-responders, from post-TT recordings (but not from pre-TT recordings)	
(Khoo et al., 2016)	16 D-iNPH, 15 NC	75.1 ± 5.3 y 44 % M	rsfMRI	ICA dual-regression scores	- iNPH-NC (**DMN**)	• ↓ DMN FC, with particular involvement of the **PCC**	• stronger DMN FC correlated with worst c-INPHGS, i-INPHGS and FAB, but not with g-INPHGS scores
(Lenfeldt et al., 2008)	11 iNPH	72. (63-82) y 64% M	fMRI	cortical activation during motor (finger tapping and reaction time) and cognitive (memory and attention) tasks	- iNPH pre/post-ELD (cortical regions associated with task execution (**SMA**))	• ↑ activation of **SMA** during motor task after ELD, associated with improvement of motor performances	• no improvement of cognitive performances after ELD (related cortical activation changes were not addressed)
(Nardone et al., 2019)	20 p-iNPH 20 NC	73.6 ± 8.1 y 60 % M	TMS	RMT, SAI	- iNPH-NC (**somatosensory cortex**)	• ↑ SAI (ie, lower inhibition of the peripheral conditioned motor response after TMS) • in patients, larger SAI correlates with worst gait and cognitive scores	
(Ogata et al., 2017)	11 iNPH 11 NC	78.2 ± 6.8 y 45 % M	rsfMRI	FC (linear correlation)	- iNPH-NC (whole brain)	• **temporal pole, orbitofrontal, medial frontal, SMA, HPC, INS FC and inter-hemispheric**FC contribute to iNPH/NC classification	• FC contains information on the severity of cognitive and urinary symptoms, but not of gait symptoms

(*continued on next page*)

Table 1 (*continued*)

Study	Sample	Demographics of iNPH patients	Imaging	Brain connectivity or activity measure(s)	Main research question(s) and regions of interest	Key positive findings	Key negative findings
(Sand et al., 1994)	11 iNPH 13 NC	64.4 (41–80) 54% M	EEG	band power content (electrode level)	- iNPH-NC - iNPH pre-/post-TT (occipito-parietal region)	• higher δ, ϑ, α baseline power (ie, EEG slowing) correlates with higher CSF outflow resistance in iNPH	• no iNPH-NC baseline EEG differences • no EEG changes after TT • no relationship between EEG pre-/post-TT changes and gait or cognitive parameters
(Seo et al., 2014)	26 p-iNPH	73.5 ± 5.5 y 69 % M	EEG	band power content (electrode level)	- iNPH TT responders/non-responders (whole brain)	• ↓baseline α2 power in **right frontal, central gyri, temporal regions** in responders compared to non-responders • higher δ2 power in **parietal and central areas**correlates with worst c-INPHGS; higher ϑ1 power in **parietal and occipital areas**with worst g-INPHGS; higher δ1 power in **frontal areas**with worst i-INPHGS, when pooling responders and non-responders)	
(Zaaroor et al., 1997)	20 iNPH 16 NC	72.0 (49–82) y 46% M	TMS	CMCT	- iNPH-NC - iNPH pre-/post-shunting	• ↓CMCT (pre- and post-shunting) in patients who did not improved gait performance after shunting (4/20), compared to NC	• normal CMCT (pre- and post-shunting) in patients who improved gait performance after shunting, compared to NC
Structural connectivity studies							
(Hattingen et al., 2010)	11 s-/p-iNPH 10 NC	76.8 ± 7.8 y	DWI (DTI)	FA, MD	- iNPH-NC (TBSS)	• ↓ FA in **CC**, ↑ FA in **periventricular CST** in iNPH compared to NC • ↑ MD in **CC** in iNPH compared to NC • higher MD in **CST** correlates with worst gait and cognitive scores in iNPH • higher FA in **CST** correlates with better gait and cognitive performance	• no correlation between CC connectivity measures and gait or cognitive scores
(Hattori et al., 2012a)	20 p-iNPH 20 NC	77.0 ± 5.1 y 40% M	DWI (DTI)	FA, D_{axial}, D_{radial}, MD	- iNPH-NC (TBSS, TSA: **CST**)	• ↑FA, MD, D_{axial} in **periventricular CST** in iNPH compared to NC • ↓FA and ↑MD, D_{radial} in **CC and juxtacortical frontal white matter** in iNPH compared to NC	
(Hattori et al., 2012b)	22 p-iNPH 20 NC 20 probable AD	77.3 ± 4.9 y 45% M	DWI (DTI)	FA, tract morphology	- iNPH-AD-NC (TSA: **FNX**)	• ↓FA in **FNX** in iNPH compared to NC and AD • **FNX** is stretched in the anteroposterior direction in iNPH compared to NC and AD (↓ FNX volume, diameter, ↑FNX length in iNPH)	
(Hattori et al., 2011)	18 p-iNPH 19 NC 11 probable AD 11 probable PD	77.3 ± 4.7 y 39% M	DWI (DTI)	FA, D_{axial}, D_{radial}	- iNPH-AD-PD-NC (TSA: **CST**)	• ↑FA, D_{axial} in **CST** in iNPH compared to NC, AD and PD (also when taking into account the amount of ventricular enlargement)	• no alterations of D_{radial} in CST in iNPH compared to NC, D_{axial}, PD
(Irie et al., 2017)	19 d-iNPH 12 NC	76.0 (67-86) y 47% M	DWI (DTI, NODDI)	FA, MD, ODI, isotropic volume fraction, intra-cellular volume fraction	- iNPH-NC (TSA: **periventricular CST**)	• ↓ODI, intra-cellular volume fraction, ↑FA, MD in **CST** in iNPH compared to NC	• no iNPH-NC differences of isotropic volume fraction
(Jurcoane et al., 2014)	26 p-iNPH 10 NC	72.4 (65–82) y 69% M	DWI (DTI), MTR, TMS	FA, D_{axial}, D_{radial}, MD, MTR, central motor conduction time	- iNPH ELD responders/ non-responders - iNPH pre/post-ELD - iNPH pre/post shunt (TSA: **CST**, **SLF**, **motor cortex**)	• ↑baseline D_{axial} in **CST** in responders and non-responders compared to NC • ↓D_{axial} in **CST** post-ELD compared to baseline in responders only • ↓D_{axial}, FA in **CST** pos-shunt compared to baseline in responders only (without reaching the NC range) • higher baseline D_{axial} in **CST** predicts better shunt outcome	• normal baseline central motor conduction time in iNPH • no pre/post-ELD or shunt changes of MTR or central motor conduction time
(Kamiya et al., 2017)	10 d-iNPH 14 NC	75.3 ± 5.1 y 30% M	DWI (DTI, NODDI, DKI)	FA, D_{axial}, D_{radial}, MD, AWF_{NODDI}, ODI_{NODDI}, AWF_{DKI}, ODI_{DKI}	- iNPH-NC - iNPH pre/post-shunt (TSA: **periventricular CST**)	• ↓baseline ODI_{DKI}, ODI_{NODDI}, ↑Daxial in iNPH compared to NC	• no pre/post-shunt changes of AWF_{NODDI}

(*continued on next page*)

Table 1 (*continued*)

Study	Sample	Demographics of iNPH patients	Imaging	Brain connectivity or activity measure(s)	Main research question(s) and regions of interest	Key positive findings	Key negative findings
						• ↓ AWF_{NODDI} in iNPH compared to NC: this effect partially explains the alterations observed in the other diffusion metrics • ↑ODI_{DKI}, ODI_{NODDI}, ↓Daxial after shunt (assessment performed 3 to 17 months after surgery)	
(Kamiya et al., 2016)	29 p-iNPH 14 NC	76.4 ± 4.9 45% M	DWI (DTI, DKI)	FA, D_{axial}, D_{radial}, MD, KI	- iNPH-NC (TBSS)	• ↑FA in **SLF, PLIC**; ↓FA in **CC, fronto-parietal connections** in iNPH compared to NC • ↑D_{axial} in **internal capsule**, ↑D_{radial} in **subcortical areas** in inPH compared to NC • ↓mean KI in **SLF, internal capsule, IFO, ILF, CC, cingulum** in iNPH compared to NC • higher FA and KI correlate with better cognitive performance (spatially unspecific effect)	• no major correlations were found between D_{axial}, D_{radial}, MD and cognitive scores
(Kang et al., 2016a)	28 p-iNPH 28 AD 20 NC	74.0 ± 3.5 y 68% M	DWI (DTI)	FA, MD	- iNPH-AD (TBSS)	• ↓FA, ↑MD in **anterior corona radiata, CC, SLF, PTR, external capsule, cerebellar peduncle** in iNPH compared to AD • lower FA in **CC and external capsule** correlates with worst gait performances	
(Kang et al., 2016b)	54 p-iNPH	74.1 ± 4.7 y 70% M	DWI (DTI)	FA, D_{axial}, D_{radial}, MD	- iNPH TT responders/non-responders (TSA: 20 fiber tracts)	• ↑ baseline FA, ↓ D_{axial}, D_{radial}, MD in **ATR, ILF, cingulum-HPC tract** in responders compared to non-responders (tests did not survive Bonferroni correction) • higher FA in **ATR, CST, ILF, IFO** correlates with less severe Parkinsonian motor symptom	• no correlations were found between DTI measures and INPHGS or classical gait measures including the TUG and 10 m walking tests
(Kanno et al., 2017)	28 iNPH	75.8 ± 4.8 y 68% M	DWI (DTI)	FA, MD	- iNPH-NC - iNPH pre/post-shunt, in shunt responders and non-responders (TBSS)	• ↓baseline FA, ↑MD in **cingulum, CC, subcortical white matter**, in responders compared to NC • ↑FA in **corona radiata** after shunt, in responders only (assessment performed 1 year after surgery)	• no baseline FA, MD differences in non-responders compared to NC • no pre/post FA, MD changes in non-responders
(Koyama et al., 2013)	24 p-iNPH 21 NC	76.3 ± 5.1 y 50% M	DWI (DTI)	FA	- iNPH-NC (TBSS)	• ↓FA in **CC, apical part of CST** in iNPH compared to NC • lower FA in CC correlates with worst gait disturbances	• no FA alterations in the cerebral peduncle • no correlations between FA and cognitive or urinary impairments
(Marumoto et al., 2012)	10 d-/p-iNPH 18 PD 10 NC	73.9 ± 2.2 y	DWI (DTI)	FA	- iNPH-PD (TSA based on DTI-81 atlas: **ATR**, $\mathbf{F_{maj}}$, $\mathbf{F_{min}}$, **CST**, **SLF**)	• ↓FA in all tracts in iNPH compared to PD (particularly in the frontal lobe) • lower FA in **ATR** correlates with increased TUG time in both iNPH and PD • FA values in **ATR** contribute to iNPH/PD discrimination in early clinical stages	• no correlations between Evan's index and tracts' FA in iNPH or PD
(Nakanishi et al., 2013)	11 p-iNPH 6 NC	73.6 (65–84) y	DWI (DTI, DKI)	FA, D_{axial}, D_{radial}, MD, KI	- iNPH-NC (TSA: **periventricular CST**)	• ↑FA, D_{axial}, MD in **periventricular CST** in iNPH compared to NC • ↓mean and axial KI in **periventricular CST** in iNPH compared to NC	• no alterations of D_{radial} or radial KI in periventricular CST
(Saito et al., 2019)	9 iNPH 8 NC	76.8 ± 4.1 y 33% M	DWI (DTI, FWI)	FA, D_{axial}, D_{radial}, MD, FW	- iNPH-NC - iNPH pre/post-shunt (TBSS, TSA: **ATR**)	• ↑baseline D_{axial}, D_{radial}, MD, FW, ↓FA in iNPH compared to NC (spatially extended effect) • ↑baseline FA in **periventricular CST** in iNPH compared to NC • ↓FA, ↑D_{radial} in **periventricular white matter, PLIC, CC** after shunt • ↓ventricle volume after shunt	• no correlation between pre-/post-shunt differences of D_{axial}, D_{radial}, MD, FW, and neuropsychological scores • no pre/post-shunt changes of diffusion metrics in ATR

(*continued on next page*)

Table 1 (*continued*)

Study	Sample	Demographics of iNPH patients	Imaging	Brain connectivity or activity measure(s)	Main research question(s) and regions of interest	Key positive findings	Key negative findings
(Younes et al., 2019)	9 iNPH 13 AD 20 NC	77.2 ± 8.6 y 44% M	DWI (DTI)	FA, D_{axial}, D_{radial}, MD, ventricular volume	- iNPH-ALZ-NC (TSA: **STR**, **CST**, **DTT**)	• FA increase in **ATR** after shunt correlates with improvement of cognitive scores • in NC, higher MD and D_{axial} in **STR, CST, DTT** correlate with larger ventricular volume • in iNPH, higher D_{axial} in **CST** correlates with larger ventricular volume • in AD, higher FA in **DTT** correlates with larger ventricular volume	
Covariance network studies							
(Yin et al., 2018)	33 p-iNPH 33 NC	65.5 ± 9.0 y	sMRI	structural covariance of grey matter volumes	- iNPH-NC (whole brain)	• ↑ network modularity in iNPH compared to NC • ↓ betweenness centrality of **orbitofrontal, INS, PCC, temporal nodes**in iNPH compared to NC	• no iNPH/NC differences of network path length and clustering coefficient

SAMPLE - ***AD***: Alzheimer's disease; ***iNPH***: idiopathic normal pressure hydrocephalus (***d-*** definite, ***p-*** probable, ***s-*** possible or suspected), according to the International iNPH Guidelines (Relkin et al., 2005) or Japanese Clinical Guidelines for iNPH (Mori et al., 2012); ***NC***: normal control; ***PD***: Parkinson disease.

DEMOGRAPHICS – ***y***: years of age; ***M***: males. When statistics were separately reported for distinct groups, pooled mean and standard deviation were computed (no differences were reported between patient subgroups within single studies).

IMAGING - ***DWI***: diffusion weighted imaging (general nomenclature, independent from the reconstruction and acquisition scheme); ***DTI***: diffusion tensor imaging; ***DKI***: diffusion kurtosis imaging; ***EEG***: electroencephalography; ***FWI***: free water imaging; ***MTR***: magnetization transfer ratio; ***NODDI***: neurite orientation dispersion and density imaging; ***rsfMRI***: resting state functional MRI; ***sMRI***: structural MRI; ***TMS***: transcranial magnetic stimulation.

BRAIN CONNECTIVITY OR ACTIVITY MEASURES – ***AWF***: axonal water fraction; ***CSD***: current source density (Kamarajan et al., 2015); D_{axial}: axial diffusivity; D_{radial}: radial diffusivity; ***FA***: fractional anisotropy; ***FW***: fractional volume of free water; ***ICA***: independent component analysis; ***KI***: kurtosis index; ***MD***: mean diffusivity; ***NPV***: normalized power variance; ***ODI***: orientation dispersion index.

MAIN RESEARCH QUESTIONS – ***CMCT***: central motor conduction time; ***ELD***: external lumbar drainage; ***RMT***: resting motor threshold; ***RSN***: resting state network; ***SAI***: short latency afferent inhibition; ***SICI***: short interval intracortical inhibition; ***TBSS***: tract-based spatial statistics; ***TSA***: tract-specific analysis; ***TT***: CSF tap test.

KEY FINDINGS - ***FC***: functional connectivity; ***INPHGS***: iNPH grading scale, including a total score and symptom-specific scores (***g-INPHGS*** for gait impairments, ***i-INPHGS*** for urinary incontinency, ***c-INPHGS*** for cognitive impairments) (Kubo et al., 2008); ***RSN***: resting state network; ***SC***: structural connectivity; ***TUG***: Timed Up and Go test.

WHITE MATTER TRACTS, GREY MATTER REGIONS AND BRAIN CIRCUITS - ***ATR***: anterior thalamic radiation; ***CC***: corpus callosum; ***CST***: corticospinal tract; ***DMN***: default mode network; ***DLPC***: dorsolateral prefrontal cortex; ***DTT***: dentatothalamic tract (connecting the dentate nucleus in the cerebellum with the thalamus); F_{maj}: forceps major; F_{min}: forceps minor; ***FNX***: fornix; ***HPC***: hippocampus; ***IFO***: fronto-occipital fasciculus; ***ILF***: inferior longitudinal fasciculus; ***INS***: insula; ***PCC***: posterior cingulate cortex; ***PCUN***: precuneus; ***PLIC***: posterior limb of the internal capsule; ***SMA***: supplementary motor area; ***SLF***: superior longitudinal fasciculus; ***STR***: superior thalamic radiation (connecting the ventral thalamic nuclei with pre- and post-central gyri).

and Puce, 2017). Alterations of resting-state cortical rhythms are a sign of pathological aging. For example, slowing down of cortical oscillations (i.e., an increase of power content in the lowest frequency bands) has been observed in Alzheimer's disease and relates to the severity of cognitive impairments (Babiloni et al., 2006). Although EEG power and current densities are not actual measures of functional connectivity, they have been related to fMRI functional connectivity values (Chang et al., 2013; Tagliazucchi et al., 2012) and functional network metrics (Demuru et al., 2020), suggesting a link between power and connectivity dimensions.

Other forms of brain connectivity are the effective connectivity, where the directionality of neural interactions is estimated from functional data with specific statistical models (Friston, 2011), and the structural covariance, where the strength of a connection between two brain regions is defined as the covariance of regions' morphological properties (e.g., cortical volume) across a population (Seeley et al., 2009). To our knowledge, no study investigated effective connectivity in iNPH. One study analyzed structural covariance networks of iNPH patients and controls (Yin et al., 2018) (Table 1).

3.1.2. Structural connectivity features of iNPH

From a structural connectivity perspective, white matter characteristics differ between iNPH patients and healthy older adults in periventricular, frontal and temporal brain circuits. These areas demonstrate spatially distinct patterns of DWI metrics' alterations, suggestive of multiple underlying neurobiological processes and distinguishing iNPH from other neurodegenerative disorders.

The most consistent finding across studies is a microstructural alteration of the corticospinal tract (CST). In the periventricular section of the CST, FA, MD and D_{axial} (but not D_{radial}) are increased (Hattingen et al., 2010; Hattori et al., 2011, 2012a; Jurcoane et al., 2014; Kamiya et al., 2016; Saito et al., 2019) and the orientation dispersion index and diffusion kurtosis are decreased (Irie et al., 2017; Kamiya et al., 2017; Nakanishi et al., 2013) (Table 1 – *Structural connectivity studies*). These effects may result from the mechanical force exerted by the enlarged lateral ventricles onto the surrounding tissues. An increase of FA, D_{axial} and orientation coherence would suggest a hyper-alignment and compression of the corticospinal fibers in the periventricular area. On the other side, the upper section of the CST and the corpus callosum show decreased FA and increased D_{radial} (but not D_{axial}) (Hattori et al., 2012a; Kamiya et al., 2016; Kang et al., 2016a; Koyama et al., 2013; Saito et al., 2019), which may reflect a stretching and fanning of white matter fibers as a consequence of ventriculomegaly. However, few studies have directly investigated the relationship between white matter microstructure and ventricle (or tract) morphometry. A single study found a relation between periventricular D_{axial} and ventricular volume in iNPH and healthy older adults (Younes et al., 2019). A study highlighted a reduction of ventricular volume and an increase of periventricular FA after CSF shunt surgery (Saito et al., 2019), but another study did not find any correlation between the FA of different white matter tracts and the Evans' index (Marumoto et al., 2012).

Besides tissue mechanical compression, other neurobiological mechanisms may contribute to the observed, spatially heterogenous structural-connectivity alterations. Frontal white matter, fronto-thalamic and fronto-parietal connections including the superior longitudinal fasciculus and the anterior thalamic radiation show decreased FA and increased MD in iNPH (Kamiya et al., 2016; Kang et al., 2016a; Marumoto et al., 2012; Saito et al., 2019), which could indicate neural degeneration, myelin impairments and/or interstitial edema. A study using free water imaging found that the anisotropy decrease/diffusivity increase in the anterior thalamic radiation were explained by changes of the free water volume fraction, suggesting presence of interstitial edema (Saito et al., 2019). On the other side, normal values of the magnetization transfer ratio indicate preserved myelin content in the periventricular CST (Jurcoane et al., 2014).

A single study investigated whole-brain network topological features of grey-matter volume covariance networks in iNPH subjects and healthy controls (Yin et al., 2018) (Table 1 – *Covariance network studies*). The study found higher global network modularity and network decentralization of functional hubs including the insula, posterior cingulate and orbitofrontal cortices.

3.1.3. Functional connectivity and activity features of iNPH

Literature investigating iNPH with functional neuroimaging technique (fMRI, EEG, TMS), is relatively sparse. Studies demonstrate functional connectivity alterations spanning multiple frequency scales and brain circuits, including inter-hemispheric, frontal, occipital, default mode network (DMN) and motor network connectivity, although findings are poorly consistent.

Functional connectivity values can be used to train machine learning algorithms and classify patients or clinical dimensions (Richiardi et al., 2013, 2011). One whole-brain fMRI study fed a linear Support Vector Machine classifier with functional connectivity values between 90 cortical regions, with the aim of classifying iNPH patients and controls, or iNPH patients with different levels of gait, cognitive and urinary symptoms (Ogata et al., 2017) (Table 1 - *Functional connectivity and activity studies*). Inter-hemispheric connections (in particular, between precentral and postcentral gyri), temporal, and anterior/posterior cingulate connections (part of the DMN (Greicius et al., 2003; Raichle, 2015)) contributed to the iNPH-control classification. A second resting-state, hypothesis-driven fMRI study showed reduced DMN connectivity in iNPH, with a particular involvement of the posterior cingulate cortex and the precuneus (Khoo et al., 2016). A tendency towards iNPH functional dysconnectivity is confirmed at shorter temporal scales by an EEG study showing decreased occipital functional connectivity in the alpha frequency band (Aoki et al., 2019).

EEG power and current density values are altered in iNPH. A slowing down of EEG signals in iNPH correlates with increased CSF outflow resistance, although this effect may relate to the patients' age (not tested) (Sand et al., 1994). Beta-band temporal power variance in frontal brain regions is increased in iNPH (Aoki et al., 2015). One study suggests that higher current source density after CSF tap test predicts positive response to shunt surgery (Ikeda et al., 2015), but another study did not find any EEG change after CSF tap test (Sand et al., 1994).

Finally, three TMS studies investigated the excitability and conduction properties of the corticospinal motor pathways (with single-pulse experiments) and intracortical inhibitory connectivity (with conditioning tests). Results indicate that gait impairments in iNPH are not related to conduction impairments of the corticospinal tract (Chistyakov et al., 2012; Jurcoane et al., 2014; Zaaroor et al., 1997). However, iNPH patients show reduced corticospinal excitability and decreased intracortical inhibitory connectivity in frontal and primary motor areas, suggesting a functional impairment of GABAergic and cholinergic neural circuits (Chistyakov et al., 2012; Nardone et al., 2019).

3.1.4. iNPH symptom triad

Approximatively half of the studies included in this review investigated possible relationships between iNPH neuroimaging outcomes and clinical symptoms (Table 1). Absence of reports may indicate negative findings. Gait impairments were associated with structural alterations of the CST, corpus callosum and frontal white matter, and functional alterations of inter-hemispheric, frontal, temporal, medial and parietal connections. Brain circuits of gait and cognitive symptoms partially overlapped, but cognitive impairments, as well as urinary symptoms, were also associated with DMN and fronto-subcortical dysconnectivity. Importantly, the spatial location and direction of the effects were poorly consistent across studies, so that it was not possible to univocally identifying the brain circuits of iNPH symptoms.

Gait impairment is the most common and earliest symptom of iNPH, and walking tests are fundamental instruments to assess clinical responses to CSF drainage and shunt surgery. Higher MD and lower FA in

the CST, anterior thalamic radiation and corpus callosum have been associated with worst gait performances in iNPH patients (Hattingen et al., 2010; Kang et al., 2016a; Koyama et al., 2013; Marumoto et al., 2012). However, another study did not find any correlation between FA in the CST, anterior thalamic radiation or fronto-temporal tracts, and gait impairments (Kang et al., 2016b). FA alterations in the CST are spatially heterogeneous, with increased anisotropy in the periventricular area (Irie et al., 2017), decreased anisotropy in the juxtacortical white matter (Saito et al., 2019), and normal values at the level of the cerebral peduncle (Koyama et al., 2013). This heterogeneity, combined with differences in region-of-interest selection, could underlie discrepancies across studies in terms of correlations between neuroimaging and clinical measures. While early reports conceptually linked gait disturbances to pyramidal tract demyelination and axonal loss (Yakovlev, 1947), TMS studies contradict this hypothesis by showing that patients responding to shunt surgery have normal CST conduction time from the motor cortex to the lower limbs (Zaaroor et al., 1997). Gait symptoms have also been related to dysfunctions of intracortical GABAergic and cholinergic inhibitory circuits in frontal motor areas (Chistyakov et al., 2012; Nardone et al., 2019), and theta and alpha EEG power in the medial and the parieto-occipital cortical regions (Aoki et al., 2013; Seo et al., 2014). One EEG study observed a relationship between gait improvement after CSF tap test and decreased alpha power variance in frontal areas (Aoki et al., 2013).

Gait and cognitive performances are interrelated in iNPH (Miyoshi et al., 2005) as well as in normal aging and neurodegenerative conditions (Morris et al., 2016; Valkanova and Ebmeier, 2017). Intracortical inhibitory dysconnectivity and frontal loss of alpha power have been related to both gait and cognitive impairments in the same studies (Aoki et al., 2013; Hattingen et al., 2010; Nardone et al., 2019). However, others found correlations between structural or functional brain connectivity features and motor, but not cognitive or urinary symptoms (Kang et al., 2016b; Koyama et al., 2013; Lenfeldt et al., 2008). Two resting-state fMRI studies associated DMN and fronto-temporal functional dysconnectivity with cognitive and urinary, but not motor symptoms (Khoo et al., 2016; Ogata et al., 2017).

Cognitive impairments correlate with white matter microstructural properties in fronto-subcortical circuits: one study found that recovery of FA in the anterior thalamic radiation one year after shunt surgery correlates with cognitive improvement (Saito et al., 2019). In probable iNPH patients, higher FA and kurtosis -but not diffusivity- in fronto-parietal and fronto-subcortical connections correlates with better cognitive performances (Kamiya et al., 2016).

Only two studies found a relationship between urinary incontinence and functional connectivity in the cingulate, insula and frontal areas (Ogata et al., 2017; Seo et al., 2014). Absence of reports may be due to difficulties in quantifying urinary symptoms.

3.1.5. Short- and medium-term plasticity mechanisms

Five functional and four structural neuroimaging studies investigated short- or medium-term brain plasticity mechanisms in iNPH patients (Table 1). They compared neuroimaging features before and after CSF tap test, external lumbar drainage, and/or shunt surgery, while differentiating responders from non-responders (i.e., patients with or without post-treatment improvement in at least one symptom domain). Structural connectivity changes in the CST track short- and medium-term plasticity mechanisms in relation to treatment response. Functional studies identify short-term changes in the frontal motor area, but negative and contradictory findings were also reported.

There was no short-term change of EEG resting-state connectivity or power content in iNPH patients after CSF tap test (Aoki et al., 2019, 2013; Sand et al., 1994), although alpha power variance was decreased in responders and tended to normalize in non-responders shortly after the test (Aoki et al., 2013). FMRI activation of the SMA during finger tapping was increased after lumbar drainage only in patients with improvement of motor performances (Lenfeldt et al., 2008). This short-term plasticity effect was ascribed to the reversal of subcortical chronic ischemia after CSF drainage, with consequent restoration of periventricular pathways to and from the SMA (not tested in the study) (Lenfeldt et al., 2008). Medium-term functional plasticity mechanisms may occur at the level of frontal inhibitory circuits: a TMS study showed a normalization of Short Interval Intracortical Inhibition values one month after shunt surgery in patients with gait improvement (Chistyakov et al., 2012).

Diffusion weighted imaging studies demonstrate long-/medium-term, and even short-term partial reversibility of white-matter alterations after treatment. FA and D_{axial} in the periventricular corticospinal tract tend to normalize (decrease) already few hours after CSF lumbar drainage (Jurcoane et al., 2014). A similar effect is still visible few months and up to one year after shunt surgery in responders only (Kamiya et al., 2017; Saito et al., 2019). A study reported increased FA in the corona radiata one year after CSF shunt surgery in responders only (Kanno et al., 2017). These findings highlight the link between symptom reversibility and white matter restoration through reversible neurobiological mechanisms, such as mechanical decompression of white matter tracts and blood flow recovery in periventricular areas.

Early, reversible iNPH pathophysiological mechanism may be followed by progressive, non-reversible processes leading to axonal loss and permanent damage. A study using advanced DWI techniques found decreased axonal density and increased fiber orientation coherence in the corticospinal tract in iNPH patients compared to healthy controls (Kamiya et al., 2017). Months after CSF shunting, the fiber orientation coherence tended to normalize, whereas the axonal density remained low, suggesting the presence of both reversible and irreversible brain damages. A possible relationship between neuroimaging findings and the duration of the pathology was not assessed in this study. Patients with impaired corticospinal conduction time, suggestive of permanent neural loss or demyelination, do not respond to shunt surgery (Zaaroor et al., 1997).

While several authors have investigated possible brain-connectivity predictors of treatment response, no accurate and reproducible iNPH prognostic marker has been identified at present (Aoki et al., 2015, 2013; Ikeda et al., 2015; Jurcoane et al., 2014; Kang et al., 2016b; Kanno et al., 2017; Seo et al., 2014).

3.2. Part 2 – Brain circuits of iNPH symptoms

We performed three ALE meta-analyses of functional contrasts evaluated on healthy populations, and directly related to iNPH symptoms, namely, locomotion, micturition and cognition (executive function). The union and intersection of the ALE maps were then investigated to identify brain circuits likely vulnerable to iNPH pathophysiology.

3.2.1. Locomotion

22 experiments comprising 369 subjects and 45 contrasts were included in this meta-analysis and reported 526 activation foci for actual or imagined locomotion tasks. A complete list of the included reference and a GingerALE-compatible text file with the MNI coordinates of activation foci are provided as supplementary documents (SI1, SI4). Demographic information for the studies included in the meta-analyses is reported in SI5. Convergence of activation foci was found in 18 grey matter clusters located in frontal, cerebellar, limbic and basal ganglia regions (Fig. 2A). The largest cluster corresponded to the bilateral supplementary motor areas (SMA), Broadman Area (BA) 6, with a predominant activation in the left hemisphere. The following clusters (ordered by size and ALE probability values) were located in the bilateral superior cerebellar vermis, anterior insula (aINS) (BA13), ventrolateral prefrontal cortex (VLPFC) (BA47), right dorsolateral prefrontal cortex (DLPC) (BA9), left dorsal striatum (putamen), globus pallidus, and thalamus. Smaller clusters were located in the right supramarginal gyrus, at the level of the temporo-parietal junction, and in

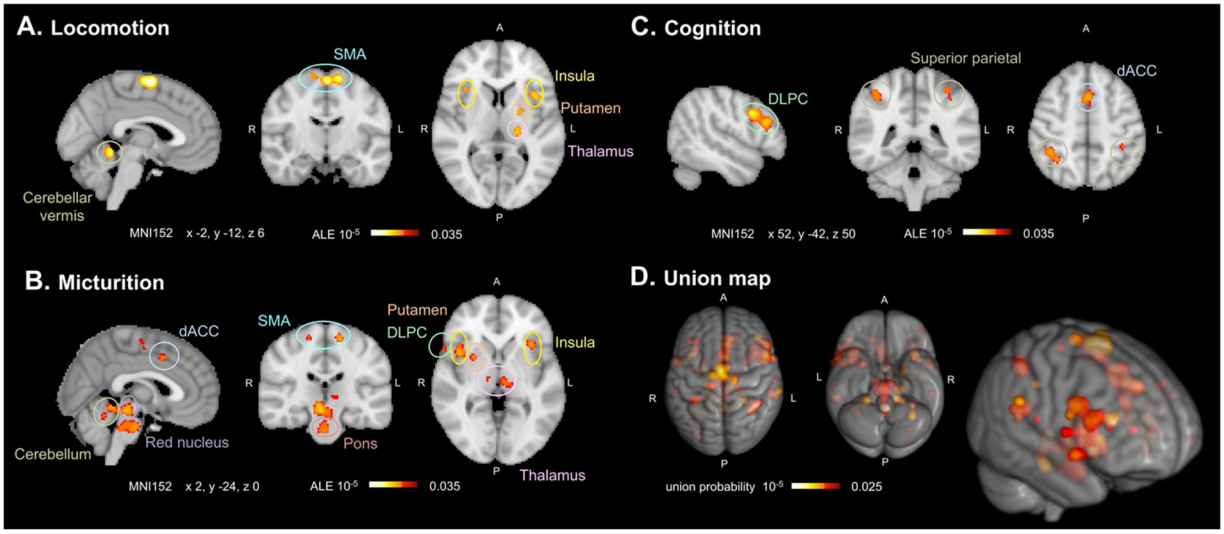

Fig. 2. Activation likelihood estimation (ALE) maps for task-based functional meta-analyses of (A) locomotion, (B) micturition, and (C) cognition (executive function tested with flanker task). Thresholded ALE values ($p < .001$, uncorrected) are overlaid to the MNI152 brain template; MNI152 coordinates of the represented brain sections are reported below each map. D. Glass-brain representation of the union of the three ALE maps, highlighting brain circuits likely to be vulnerable to iNPH pathophysiological mechanisms. SMA: supplementary motor area; dACC: dorsal anterior cingulate cortex; DLPC: dorsolateral prefrontal cortex.

the right superior parietal lobule (BA7). The results of this meta-analysis are in line with our knowledge of the central locomotion control system, which includes a fronto-subcortical-cerebellar stream responsible for steady-state gait control, gait initiation and emotional reference, and a cortical (SMA, primary motor cortex)-subcortical stream for adaptive locomotor control (Boyne et al., 2018; Takakusaki, 2017). Moreover, temporo-parietal regions are responsible for the integration of bodily information for locomotion adjustment, whereas the prefrontal cortex contributes to motor intention and planning (Takakusaki, 2017).

3.2.2. Micturition

The meta-analysis of 17 studies, including 165 subjects, 27 contrasts and 299 foci, identified 21 clusters of convergent functional activation related to micturition (SI2, SI4, SI5). The largest clusters involved regions of the cerebellum, pons, midbrain (at the level of the red nucleus, mammillary body and substantia nigra), thalamus (ventral posterior and lateral, medial dorsal nuclei), right putamen and bilateral aINS (BA13) (Fig. 2B). Frontal lobe activation converged medially in the SMA (BA6) and the left dorsal anterior cingulate cortex (dACC) (BA32), and laterally in the prefrontal cortex (pars opercularis (BA44) and the VLPFC (BA47)). The bilateral temporo-parietal cortices (BA40, BA22) were also involved. The insula, prefrontal cortex, ACC and SMA have been implicated in the perception of bladder fullness, sense of urinary urgency, and modulation of bodily arousal states and motivation linked to the voluntary control of bladder voiding (Griffiths, 2015). Cortical signals to and from these regions are relayed through the spinobulbar micturition centers, which are as well part of the micturition ALE map.

3.2.3. Cognition (executive function)

This meta-analysis was restricted to a BrainMap database search for positive activation loci with experimental paradigm class ‘Flanker’. The database search returned 17 studies including 252 subjects and 32 contrasts (SI3, SI4, SI5). The analysis of the 304 foci revealed highly symmetric activation convergence in the frontal and parietal lobes, involving the bilateral ACC (BA32, BA8), DLPC (BA9), superior parietal and supramarginal cortices (BA7, BA40), and aINS (BA13), forming 11 significant clusters (Fig. 2C). Executive attention tests, such as the flanker, are known to predominantly activate the ACC, which has been linked to conflict detection during information processing (van Veen and Carter, 2002). A fronto-parietal/cingulo-opercular network including the DLPC, ACC, aINS and the superior parietal cortices is associated with supervisory attentional control and top-down mechanisms in response to conflict (Li et al., 2017).

3.2.4. Relationship between iNPH circuits

The union probability map of the three meta-analyses is shown on a glass brain in Fig. 2D. This map represents grey matter and cerebellar areas that, in healthy subjects, are associated with at least one of the three symptoms of iNPH. The union probability map involves the medial, frontal and temporal areas including the SMA, ACC, aINS, DLPC and posterior parietal cortex. Implicated fronto-subcortical, spinobulbar and cerebellar circuits span the lateral and ventral thalamus, the dorsal striatum, the pons and the vermis.

We evaluated the intersection (minimum statistic conjunction) of meta-analytic ALE maps. Considering that, according to the international guidelines, a patient with probable iNPH should present at least two out of the three symptoms (Relkin et al., 2005), brain regions implicated in more than one meta-analysis are likely to be vulnerable ‘hotspots’ to iNPH pathophysiological mechanisms. Centroid MNI coordinates of ALE map intersections are reported in Table 2. The intersection of the three ALE maps consists of a single cluster in the left aINS (BA13), suggesting a prominent implication of this region in iNPH (Fig. 3A). The locomotion and executive function circuits intersect in the right DLPC (BA46) and medial frontal cortex. In this region, areas associated with locomotion first, and higher-order function (flanker task) then, form a posterior-to-anterior gradient of activation which spans the medial SMA and dACC (Fig. 3B). The locomotion and micturition networks overlap in the cerebellar culmen, bilateral aINS, SMA (BA6), left putamen and right BA42 (part of the auditory cortex). Finally, the micturition and executive function circuits intersect in the dACC (BA32). Regions specifically associated with individual symptoms include parts of the cerebellum (bilateral anterior lobe and left tonsil, exclusively associated with gait), brainstem areas (associated with micturition) and bilateral posterior parietal cortices (BA7, 39, 40, associated with executive functions).

Table 2
Intersection of ALE maps for locomotion, micturition and cognition (executive function tested with flanker task). The intersections between pairs of, or all the three ALE maps were assessed as minimum statistic conjunction and resulted in clusters of voxels representing the overlap between the maps. The table reports, in the order: a cluster numerical identifier; the number of voxels in the cluster (voxel size 2 × 2 × 2 mm^3, MNI152 space); the geometric centroid of the cluster in MNI152 coordinates; the lobe and anatomical region according to the Talairach daemon; the main anatomical and behavioral dimensions according to the Neurosynth database; the cytoarchitectonic Brodmann Area (BA) associated with the centroid coordinates.

Clust.	#voxels	Centroid	Lobe	Anatomical label	Neurosynth associations	BA
Locomotion AND Micturition AND Cognition						
1	9	−34, 18, 4	left sub-lobar	insula	insula (z 11.29), goal (z 12.9)	BA13
Locomotion AND Micturition						
1	63	0, -46, -10	bilateral cerebellum	culmen	cerebellum (z 4.87), serial processing (z 4.70)	–
2	18	42, 20, -4	right frontal lobe	inferior frontal gyrus	anterior insula (z 11.22), fear (z 10.91)	BA47
3	12	−34, 18, 4	left sub-lobar	insula	insula (z 11.29), goal (z 12.92)	BA13
4	11	−24, 0, 8	left sub-lobar	putamen	putamen (z 17.17), movements (z 8.26)	–
5	5	−36, 18, -4	left frontal lobe	inferior frontal gyrus	anterior insula (z 13.92), fear (z 17.25)	BA47
6	3	38, 20, 6	right sub-lobar	insula	insula (z 11.17), goal (z 8.12)	BA13
7	3	60, -34, 20	right temporal lobe	superior temporal gyrus	premotor cortex (z 7.44), action observation (z 8.24)	BA42
8	3	0, -12, 62	bilateral frontal lobe	medial frontal gyrus	supplementary motor cortex (z 13.92), movement (z 9.65)	BA6
Locomotion AND Cognition						
1	30	−36, 16, 6	left sub-lobar	insula	insula (z 11.52), goal (z 11.22)	BA13
2	8	42, 36, 20	right frontal lobe	middle frontal gyrus	lateral prefrontal (z 6.44), working memory (z 6.30)	BA46
3	8	4, -2, 60	right frontal lobe	medial frontal gyrus	motor cortex (z 17.29), movement (z 12.79)	BA6
4	1	44, 32, 24	right frontal lobe	middle frontal gyrus	dorsolateral prefrontal (z 8.43), working memory (z 9.48)	BA46
Micturition AND Cognition						
1	23	2, 10, 44	bilateral frontal lobe	medial frontal gyrus	supplementary motor (z 7.75), anterior cingulate (z 5.28), goal (z 15.72)	BA32
2	22	−34, 20, 4	left sub-lobar	insula	insula (z 13.22), goal (z 15.72)	BA13
3	1	42, 16, 10	right frontal lobe	inferior frontal gyrus	insula (z 7.98), response inhibition (z 6.46)	BA44

4. Discussion

4.1. Brain circuits of iNPH: bridging literature and meta-analytic perspectives

iNPH is a poorly understood disorder with a high prevalence in the elderly population and difficult diagnosis because of unspecific clinical symptoms, presence of comorbidities and lack of quantitative biomarkers. The ventricle enlargement and compression of periventricular tissues may engender a cascade of harmful events impacting large-scale brain circuits, ultimately causing locomotion, micturition and cognitive impairments partially reversible after treatment. A restricted number of studies has investigated the structural and functional connectivity features of iNPH and their changes in relation to symptoms and treatment (Table1). Structural connectivity analyses identify consistent and iNPH-specific patterns of white matter alterations mainly in periventricular and frontal, but also in temporal and parietal areas, which tend to normalize after treatment and to distinguish iNPH patients from those with comorbid disorders, such as Alzheimer's disease (AD). Correlations with clinical symptoms are present but discordant across studies. Functional analyses are few and highly heterogeneous in terms of neuroimaging techniques and connectivity measures. Although there is an association between functional features and iNPH clinical manifestation, the available literature does not allow to draw major conclusions on affected functional circuits. Isolated findings point out impairments of inter-hemispheric, posterior cingulate and frontal, but also parietal, temporal and occipital functional measures. Direction of the effects (e.g., increased or decreased functional connectivity and band power content), differences between treatment responders and non-responders, and relationship with symptoms are inconsistent among studies.

The iNPH symptoms' meta-analyses of brain functional activations

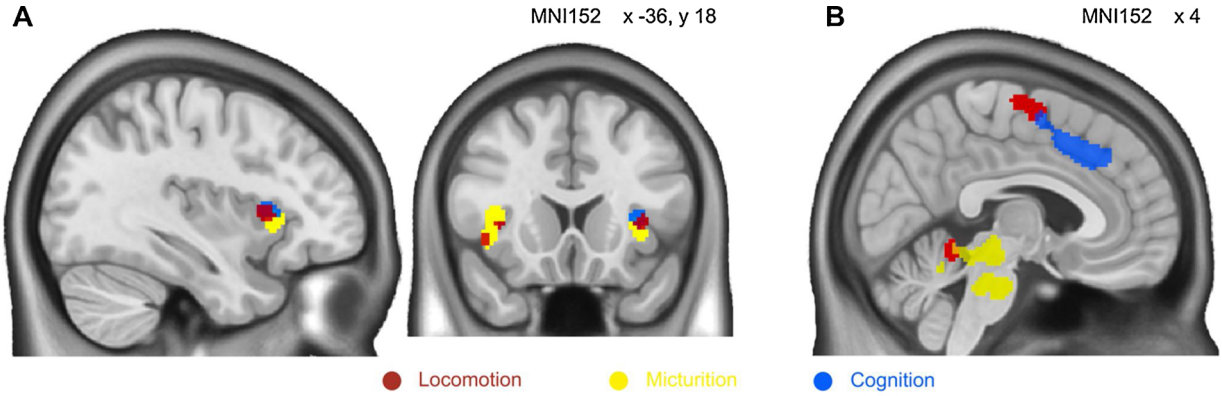

Fig. 3. Clusters representing the overlap of the of the activation likelihood estimation (ALE) maps of locomotion (red), micturition (yellow) and cognition (executive function, blue). A. The three maps intersect in the left anterior insula; the locomotion and micturition maps also intersect in the right anterior insula. B. The locomotion and cognition maps intersect in the medial frontal cortex, extending posteriorly to anteriorly from the medial SMA to the dACC; the locomotion and micturition maps overlap in the cerebellar.

in healthy populations indicate frontoparietal-subcortical-cerebellar circuits as possible basins of vulnerability to iNPH pathophysiological mechanisms (Table2, Fig. 1). The juxtaposition of the literature review and meta-analyses reinforces the conceptualization of new hypotheses on iNPH brain circuits, which we develop in the following sections.

4.1.1. Salience and attention networks

INPH literature highlights convergent structural connectivity findings in the periventricular white matter spanning motor pathways (corticospinal tract, corona radiata, superior thalamic radiation), homotopic connections (corpus callosum), the fronto-subcortical loops (anterior thalamic radiation), the fronto-parietal (superior longitudinal fasciculus), and the parieto-temporal (inferior longitudinal fasciculus) circuits (Table 1). These structural alterations converge on the frontal lobe and tap multiple cortical and subcortical regions. Among them, the *anterior insula (aINS)* emerges has a functional 'hot spot' of iNPH, representing the intersection of locomotion, micturition and executive function meta-analyses (Fig. 3A). We note that the insula plays an integrative role in the brain in general, linking information from diverse functional systems (Kurth et al., 2010) and representing a hub of central autonomic processing (Beissner et al., 2013).

Although none of the hypotheses-driven studies included in this review specifically focused on the insula, two whole-brain analyses indicated impaired structural and functional insula connectivity in iNPH (Ogata et al., 2017; Yin et al., 2018). Ablation experiments in monkeys and *in vivo* DWI tractography in humans show that insula projections traverse the corpus callosum, corona radiata, external capsule and superior/inferior longitudinal fasciculus (Ghaziri et al., 2017; Uddin et al., 2017), in agreement with the tracts demonstrating microstructural changes in iNPH.

Functionally, the aINS connects with the *dorsal anterior cingulate cortex (dACC)* and the *dorsolateral prefrontal cortex (DLPC)* (Cauda et al., 2011; Chang et al., 2013), two regions that appear in iNPH literature (Aoki et al., 2013; Kang et al., 2016b; Ogata et al., 2017) and are centrally implicated in iNPH symptoms. The dACC represents the intersection of the micturition and cognition meta-analyses, and together with the aINS, it forms the *salience network* (Menon, 2015; Seeley et al., 2007). The DLPC contributes to the locomotion and cognition meta-analyses and connects to the posterior parietal cortex through the superior longitudinal fasciculus (implicated in iNPH (Jurcoane et al., 2014; Kamiya et al., 2016)), forming the *central executive and attention networks* (Fox et al., 2006; Vossel et al., 2014).

Besides their relationship with iNPH symptoms triad, the implication of the salience and attention networks is in line with additional behavioral traits of the disorder. Behavioral disturbances including apathy and depression are highly prevalent in iNPH (Israelsson et al., 2016; Peterson et al., 2016). Apathy, a state of decreased motivation affecting goal-oriented behavior, relates to gait impairments and predicts shunt response in iNPH patients (Allali et al., 2017, 2018a,b). Brain atrophy and hypometabolism in cortical circuits involving the medial and dorsal prefrontal cortex (including dACC, DLPC and SMA) and the dorsal striatum relate to apathy severity in AD and Parkinson's diseases (PD) (Pagonabarraga et al., 2015). Possible relationships between insula connectivity features and apathy in iNPH remain to be investigated.

We conclude that the salience network and fronto-parietal attentional/executive networks, with a particular focus on the aINS, dACC and DLPC, might be particularly vulnerable to the iNPH pathophysiology and deserve specific attention in future research.

4.1.2. Locomotion networks and cognitive control

Locomotion impairment is a core symptom of iNPH and many hypothesis-driven studies focused on the corticospinal tract (CST). DWI properties of the CST are altered in iNPH compared to normal aging (Hattingen et al., 2010; Saito et al., 2019) and tend to normalize after treatment (Jurcoane et al., 2014; Kamiya et al., 2017; Kanno et al., 2017). However, the association between gait impairments and white matter features is controversial and not specific to the CST (Kang et al., 2016b; Koyama et al., 2013). Functional studies do not find main alterations of the motor network in iNPH (Aoki et al., 2019, 2015, 2013; Khoo et al., 2016; Ogata et al., 2017; Seo et al., 2014); myelin content and neural excitability of the CST are unaffected (Chistyakov et al., 2012; Jurcoane et al., 2014; Nardone et al., 2019; Zaaroor et al., 1997).

These considerations suggest that structural and functional connectivity of the primary motor network is not the only substrate of locomotion impairments in iNPH. Indeed, locomotion tasks engage cognitive control, involving movement initiation (accomplished through prefrontal cortex and limbic circuits), visuomotor information processing (posterior parietal and temporo-parietal cortices), executive functions to guide future behavior (fronto-subcortical circuits), and postural control (basal ganglia and cerebellum) (Bohnen and Jahn, 2013; Takakusaki, 2013). In normal and pathological aging (including iNPH) gait performances are associated with executive decline (Beauchet et al., 2012; Miyoshi et al., 2005; Morris et al., 2016) and locomotion increasingly relies on cognitive control, requiring a more widespread recruitment of frontal areas (Hugenschmidt et al., 2014; Scala et al., 2019; Seidler et al., 2010). In parallel, frontal areas are the main target of aging processes and become less efficient (Gunning-Dixon et al., 2009; Lustig et al., 2003). It remains to be elucidated how ventriculomegaly interferes with these processes through damage of periventricular tissues and fronto-subcortical tracts (Kang et al., 2016b; Saito et al., 2019).

One hypothesis is that, in order to compensate for brain alterations, iNPH subjects may recruit more neural resources than healthy elderly, according to a posterior-to-anterior frontal gradient that parallels an increasing complexity of executive control. A recent cascade model conceptualizes higher-order control (behavior selection and initiation) as a hierarchical process implemented by the medial and the lateral prefrontal cortices, with more complex signals (sensorimotor to contextual to episodic control) arising from successively more anterior regions (Koechlin and Summerfield, 2007; Kouneiher et al., 2009). This progression is reflected in the union and intersection of the locomotion and executive function maps derived from our meta-analyses, which defines a rostro-caudal axis from premotor/SMA to dACC areas (Fig. 3B). Future research should investigate functional activation during simple and complex imagined locomotion tasks (Van Der Meulen et al., 2014) and functional and structural connectivity features along this rostro-caudal axis, which might relate to the progression of iNPH pathology.

4.2. Brain connectivity changes in comorbid and mimic disorders

iNPH has a high prevalence of neurological comorbidities, the most frequent being AD with histological findings present in around 40 % of patients, and comorbidities are an important predictor of treatment outcome (Jang et al., 2018; Malm et al., 2013a). Moreover, iNPH symptoms are shared with other neurological disorders, such as PD and progressive supranuclear palsy (PSP), which complicates iNPH diagnosis and clinical management (Allali et al., 2016; Magdalinou et al., 2013; Malm et al., 2013a). Comparing structural and functional connectivity features characterizing iNPH, comorbid and mimic disorders is therefore of central interest.

In AD, both structural and functional connectivity alterations concentrate in the DMN, a resting-state network comprising posterior cingulate/precuneus, posterior parietal, medial temporal/hippocampal and medial prefrontal cortices (Greicius et al., 2003; Raichle, 2015). DMN hypoconnectivity and amyloid deposition are already present in preclinical AD (Palmqvist et al., 2017; Pievani et al., 2014; Sperling et al., 2009) and predict cognitive decline in older populations (Tomasi and Volkow, 2012). One of the studies included in this review found DMN hypoconnectivity in iNPH (Khoo et al., 2016), and medial components of the DMN contribute to patient-control discrimination (Ogata

et al., 2017). However, iNPH patients included in the studies did not receive CSF or PET screening for amyloid or tau deposition. One possibility is that DMN impairments in iNPH relates to (amyloid) comorbid disorders, and future research should address possible relationships between iNPH and proteinopathies (Manniche et al., 2019). The other possibility is that DMN alterations in iNPH, AD and other neurodegenerative/vascular conditions have different pathophysiological origins, which should be investigated with multi-modal studies including molecular and functional imaging.

While the clinical presentation of AD differs from iNPH, other 'mimic' neurodegenerative disorders, such as PD or PSP, share locomotion and behavioral traits with iNPH and diagnostic differentiation can be challenging (Höglinger et al., 2017). For example, in PSP cerebellar-thalamo-cortical dysconnectivity features correlate with motor symptom severity and involve the SMA, premotor cortex and striatum (Gardner et al., 2013; Pievani et al., 2014; Whitwell et al., 2011a, 2011b), indicating an overlap with brain circuits implicated in iNPH. Similarly, structural and functional connectivity alterations in cerebellar, parietal, precuneus and prefrontal cortices, superior longitudinal fasciculus, corpus callosum and corticospinal tract correlate with gait impairments in PD (Allali et al., 2018a,b). Moreover, freezing of gait in PD has been related to abnormal integration between motor and executive regions and altered functional connectivity in the dorsal attention network (Maidan et al., 2019), suggesting a reorganization of the systems devoted to the cognitive control of gait. Although the types of locomotion impairments in PD, PSP and iNPH partially differ (Selge et al., 2018; Stolze et al., 2001), there could be a common tendency to increasingly rely on frontal cognitive resources for locomotion, which has not been tested yet (see also Section 4.1.2). Future researches should investigate possibly distinct brain connectivity substrates of gait features, such as gait speed and temporal variability, to reinforce our comprehension of gait phenotypes in iNPH, PD and PSP (Verghese et al., 2013).

With the aim of identifying neuroimaging features specific to iNPH, some studies directly compared iNPH to other pathological populations, including AD and PD (Chistyakov et al., 2012; Hattori et al., 2012b, 2011; Marumoto et al., 2012; Siasios et al., 2016; Younes et al., 2019). iNPH patients show a particular DWI contrast of high fractional anisotropy and mean diffusivity in periventricular areas, and low fractional anisotropy in frontal areas, a measure that could be used in the future to reinforce the robustness of iNPH diagnostic criteria (Andersson et al., 2017). However, it is unlikely that a single neuroimaging feature could serve as iNPH biomarker. New research lines focus on transdiagnostic approaches to characterize common brain substrates of clinical and behavioral dimensions across diagnostic boundaries of neuropsychiatric disorders (Douw et al., 2019; Xia et al., 2018). These approaches leverage multivariate statistical techniques, such as partial least square or canonical correlation analysis, to jointly investigate multiple sources of clinical and neuroimaging data (Krishnan et al., 2011; Meskaldji et al., 2016). Among the latter, new methods for brain networks construction based on cortical regions' morphometric similarity mapping and proteins' deposition patterns could prove useful in the study of dementias (Ossenkoppele et al., 2019; Seeley et al., 2009; Seidlitz et al., 2018). When applied to neurodegenerative disorders and large cohorts, multivariate and multimodal techniques could serve to better characterize brain changes related to iNPH symptoms and disentangle comorbidities.

4.3. Perspectives: Pathophysiological substrate of reversible and irreversible brain changes

A fundamental aim of iNPH neuroimaging research is to help distinguishing reversible from irreversible neurobiological processes. The natural course of iNPH consists in symptom progression over time, and timing of intervention is key to successful treatment (Andrén et al., 2014). Being able to place the patient within a continuum of pathological evolution (similarly to PD staging (Braak et al., 2004)) on the basis of the amount of irreversible brain damage could improve treatment selection. The investigation of multiple diffusion-weighted magnetic resonance imaging (DWI) metrics, in combination with prognostic tests (Marmarou et al., 2005) and functional neuroimaging could bring major advances in this direction.

Different neurobiological processes, including mechanical deformation of brain tissues in periventricular areas, interstitial edema, small vessels disorders and neural loss have been implicated in iNPH pathophysiology (Keong et al., 2016; Williams and Malm, 2016). These processes affect the white-matter microstructure and can be probed with advanced DWI techniques, such as free water imaging and neurite orientation dispersion density imaging among others (Pasternak et al., 2009; Zhang et al., 2012). These techniques are nowadays compatible with clinical settings and allow quantifying biologically relevant variables, e.g., axonal density, axonal diameter, fraction of unconstrained water and tract morphology (Daducci et al., 2016; Panagiotaki et al., 2012; Winston, 2012). For example, one recent study assessed the fiber orientation coherence and axonal density of the corticospinal tract before and after shunt surgery in iNPH patients (Kamiya et al., 2017). The fiber orientation coherence tended to normalize after surgery, indicating a decompression of the tract, but the axonal density remained impaired, suggesting irreversible neural losses. Further multi-modal studies are required to link these changes to pathophysiological and molecular pathways. For example, TMS has emerged as a promising technique to assess motor cortical function in various neurodegenerative disorders and tracking their progression (Ahmed et al., 2018; Vucic and Kiernan, 2017). The investigation of structural and functional properties of the motor network/corticospinal tract with DWI and TMS may provide a fine-grain characterization of disease stages.

We can hypothesize that different brain circuits may be concerned by multiple neurobiological processes in different proportions and at different moments over the evolution of the pathology, leading to spatially and temporally heterogenous patterns of multi-contrast DWI changes in the white matter (Hattori et al., 2012a; Kamiya et al., 2016). This feature is highly relevant for iNPH differential diagnosis and highlights the importance of a circuit-level perspective for a better comprehension of reversible and irreversible processes. For example, one may expect that early compression of nervous fibers in periventricular areas precede later irreversible neurodegeneration in the same and frontal brain areas. To appreciate these changes, it is fundamental to achieve a robust and quantitative characterization of white matter circuits, even where those circuits partially overlap in space. New DWI processing methods, such as microstructure-informed tractography, higher-order diffusion models and tract-based morphometry, can disentangle the microstructural properties of multiple nervous bundles passing through the same white matter voxels and pinpoint tract-specific alterations (Girard et al., 2017; OöDonnell et al., 2009; Raffelt et al., 2017). These methods have recently been used to characterize tract-specific patterns of white matter alterations in mild cognitive impairment and AD (Mito et al., 2018). In iNPH, they could for example be used to extract microstructural markers along the corticospinal tract in relation to the distance from the lateral ventricles (Hattori et al., 2012a), which might relate to the progression of the pathology.

4.4. Perspectives: Functional characterization of iNPH networks

iNPH represents the leading cause of reversible dementia and, as such, it offers a unique opportunity to study plasticity mechanisms and functional reorganization in the aging brain at the short and medium time scales. The first structural brain changes after CSF drainage are likely to occur in periventricular areas (Jurcoane et al., 2014; Kamiya et al., 2017; Kanno et al., 2017; Saito et al., 2019) and be accompanied by a reorganization of neural communication patterns reflecting symptoms reversal. For example, white matter diffusion measures in the corticospinal tract (Jurcoane et al., 2014) and supplementary motor

areas activation during finger tapping (Lenfeldt et al., 2008) tend to normalize already few hours after CSF removal in patients responding to the intervention. Future research should extend these results by directly relating neuroimaging measures of functional reorganization to specific clinical changes.

Current functional neuroimaging approaches quantify 'static' functional connectivity in the brain by computing pair-wise signal relationships over functional recordings lasting several minutes, but they disregard the temporal fluctuations of those interactions in time (Preti et al., 2017). The latter information can be particularly relevant to the study of iNPH because it reveals short-term functional plasticity mechanisms occurring during motor learning (Bassett et al., 2015, 2011), relates to cognitive and motor impairments in AD and PD (Chen et al., 2015; Quevenco et al., 2017), and demonstrates higher accuracy in diagnostic classification compared to 'static' functional connectivity approaches (Chen et al., 2017; de Vos et al., 2018; Di Perri et al., 2018). Different methods have been recently proposed to quantify functional connectivity dynamics (Calhoun et al., 2014; Hutchison et al., 2013; Preti et al., 2017), including sliding-window approaches and single time-point analyses based on co-activation patterns, constrained deconvolution, Hilbert transform or graph Laplacian operator (Glomb et al., 2019; Karahanoğlu and Van De Ville, 2017; Liu and Duyn, 2013; Tewarie et al., 2019). These methods decompose functional recordings into sequences of states and assess their temporal characteristics and dynamic interactions.

A recent study using co-activation pattern analysis observed that reduced switching among functional states correlates with motor symptom severity in the early stages of PD (Zhuang et al., 2018). Considering that locomotion control relies on the integration of information between motor, frontal and subcortical networks (Fig. 2A), future research should investigate whether and how the interactions between these networks can be modulated by an external intervention that improves locomotion. For example, it would be interesting to analyze the neural dynamics of motor and cognitive control using EEG portable devices during motor-cognitive dual tasks (Kahya et al., 2019; Li et al., 2018), before and after shunting.

Dynamic functional connectivity analyses may also be relevant for the characterization of salience network dynamics, a circuit likely implicated in iNPH pathophysiology. Salience network nodes, including the aINS, are highly flexible and coordinate the switching between the default mode and central executive networks (Sridharan et al., 2008; Uddin, 2015). These properties correlate with executive functions in healthy subjects (Chen et al., 2016) and cognitive impairments in older adults (Chand et al., 2017). It is currently unknown whether salience network dynamics are affected in iNPH and relate to cognitive improvement after treatment; future researches should address this gap.

Finally, an important piece of research will be to relate brain functional changes to the underlying architecture of white matter connections. Many of the studies included in this review conclude with the hypotheses on the functional consequences of white matter alterations or, conversely, on the structural substrate of functional connectivity changes. Testing these hypotheses requires specific methodological settings and multimodal investigations. Recent advances in network science offer appealing mathematical frameworks for the analysis of signals (e.g., fMRI, EEG data) living on graphs (white matter structural connectivity networks), offering the possibility of studying the interplay between brain structure and function under new perspectives. For example, multilayer network models retrieve recurring patterns of brain activity propagation on the white matter network (Griffa et al., 2017). Signal processing methods applied to the graph-domain (Shuman et al., 2013) identifies local and global brain signal components with different degrees of alignment with respect to the underlying structural connectivity architecture (Petrovic et al., 2019; Preti and Ville, 2019; Shuman et al., 2016). These approaches have proved relevant for the investigation of cognitive flexibility, which is often reduced in patients with neurological conditions (Huang et al., 2018). Further developments of statistical and dynamical models on one side, and of mathematical network instruments on the other side, may help shaping a new integrated understanding of the dynamical processes evolving on brain networks in general, and contribute to the understanding of iNPH mechanisms in particular.

4.5. Technical aspects and limitations

This perspective review focused on studies investigating brain connectivity alterations in iNPH and its aim was not to provide a comprehensive survey of neuroimaging literature (to this end, we refer to (Hoza et al., 2015; Keong et al., 2016; Siasios et al., 2016; Tarnaris et al., 2009)). The review identified consistent findings across studies. However, it also pointed out several inconsistencies that can be due to several factors. First, the methodological approaches substantially differ across studies, e.g., in the way how regions of interest are selected or functional interactions are quantified. Second, the sample sizes are relatively small, with an average of 20 iNPH patients included in each study. Third, despites the elaboration of clinical and radiological guidelines, there is a lack of standardization and different healthcare structures may comply with different criteria for diagnosis, treatment selection and patients' inclusion in clinical studies. Moreover, patients did not undergo molecular screening for comorbid neurological conditions, such as AD. For these reasons, the investigated samples might be heterogeneous across studies.

The number of functional neuroimaging studies is limited and the conclusions that can be drawn are relatively limited at the moment. Only six studies investigated genuine functional connectivity features in iNPH. Studies focusing on band power and current density have been included in the review to offer a broader picture of functional analyses in iNPH. The lack of functional connectivity studies could be explained by the methodological complexity or unpublished negative results. Future research should clarify this aspect, particularly with respect to the characterization of functional plasticity mechanisms after intervention.

The literature review was complemented by a set of meta-analyses of iNPH symptoms, limited to task-based functional studies in healthy subjects only. Since the number of task-based investigations of iNPH clinical dimensions is limited, it was not possible to perform the meta-analyses on iNPH patients. Subjects included in the meta-analyses were on average younger than iNPH patients (SI5). Aging has been associated with inefficient functioning of brain circuits and compensatory over-activation mechanisms, particularly in the prefrontal cortex (Mirelman et al., 2017; Park and Reuter-Lorenz, 2009). The circuits' union and intersections identified in the meta-analyses could therefore be conservative when used to investigate older populations. The inclusion of age-matched control groups in future circuit-based neuroimaging studies remains of central importance.

5. Conclusions

We used two complementary approaches (literature review and symptoms meta-analyses) to unravel the role of different brain circuits with respect to iNPH pathophysiology. These two perspectives add compatible and complementary pieces of information to the conceptualization of iNPH connectopathy, identifying the salience network, attentional networks and a rostro-caudal axis in the medial prefrontal cortex as key circuits associated with iNPH and possible connectivity biomarkers of symptom dimensions. In particular, our considerations conceptually link locomotion impairments in iNPH to frontal cognitive control.

iNPH literature attests an important effort from both the neurology and neuroimaging communities to identify quantitative markers for iNPH differential diagnosis and prognosis. The development of accurate markers will require a better comprehension of the links between iNPH neurobiological processes and macroscale (multimodal) neuroimaging

data, which can help disentangling reversible from irreversible components of brain connectivity damages and staging the progression of the disease. We hope that a growing effort from healthcare institutions and clinical research, combined with tailored methodological development in the field of neuroimaging, will help us to further understand this complex disorder and increase the prognostic reliability and treatment options.

Declaration of Competing Interest

None.

Acknowledgments

This work was supported by the Swiss National Science Foundation [grant number #320030_173153]. We thank Maria Giulia Preti and Daniela Zöller for the insightful discussions and suggestions.

Appendix A. Supplementary data

Supplementary material related to this article can be found, in the online version, at doi:https://doi.org/10.1016/j.neubiorev.2020.02.023.

References

Ahmed, R.M., Ke, Y.D., Vucic, S., Ittner, L.M., Seeley, W., Hodges, J.R., Piguet, O., Halliday, G., Kiernan, M.C., 2018. Physiological changes in neurodegeneration — mechanistic insights and clinical utility. Nat. Rev. Neurol. 14, 259–271. https://doi.org/10.1038/nrneurol.2018.23.

Alexander, A.L., Lee, J.E., Lazar, M., Field, A.S., 2007. Diffusion tensor imaging of the brain. Neurother. J. Am. Soc. Exp. Neurother. 4, 316–329. https://doi.org/10.1016/j.nurt.2007.05.011.

Allali, G., Garibotto, V., Assal, F., 2016. Parkinsonism differentiates idiopathic normal pressure hydrocephalus from its mimics. J. Alzheimers Dis. JAD 54, 123–127. https://doi.org/10.3233/JAD-160428.

Allali, G., Laidet, M., Armand, S., Saj, A., Krack, P., Assal, F., 2017. Apathy and higher level of gait control in normal pressure hydrocephalus. Int. J. Psychophysiol. 119, 127–131. https://doi.org/10.1016/j.ijpsycho.2016.12.002. The Psychophysiology of Motivation: Body and Brain in Action.

Allali, G., Blumen, H., Devanne, H., Pirondini, E., Delval, A., Van De Ville, D., 2018a. Brain imaging of locomotion in neurological conditions. Neurophysiol. Clin., XXVe congrès SOFPEL 48, 337–359. https://doi.org/10.1016/j.neucli.2018.10.004.

Allali, G., Laidet, M., Armand, S., Assal, F., 2018b. Brain comorbidities in normal pressure hydrocephalus. Eur. J. Neurol. 25, 542–548. https://doi.org/10.1111/ene.13543.

Andersson, J., Rosell, M., Kockum, K., Söderström, L., Laurell, K., 2017. Challenges in diagnosing normal pressure hydrocephalus: evaluation of the diagnostic guidelines. eNeurologicalSci 7, 27–31. https://doi.org/10.1016/j.ensci.2017.04.002.

Andrén, K., Wikkelsø, C., Tisell, M., Hellström, P., 2014. Natural course of idiopathic normal pressure hydrocephalus. J. Neurol. Neurosurg. Psychiatry 85, 806–810. https://doi.org/10.1136/jnnp-2013-306117.

Aoki, Y., Kazui, H., Tanaka, T., Ishii, R., Wada, T., Ikeda, S., Hata, M., Canuet, L., Musha, T., Matsuzaki, H., Imajo, K., Yoshiyama, K., Yoshida, T., Shimizu, Y., Nomura, K., Iwase, M., Takeda, M., 2013. EEG and Neuronal Activity Topography analysis can predict effectiveness of shunt operation in idiopathic normal pressure hydrocephalus patients. Neuroimage Clin. 3, 522–530. https://doi.org/10.1016/j.nicl.2013.10.009.

Aoki, Y., Kazui, H., Tanaka, T., Ishii, R., Wada, T., Ikeda, S., Hata, M., Canuet, L., Katsimichas, T., Musha, T., Matsuzaki, H., Imajo, K., Kanemoto, H., Yoshida, T., Nomura, K., Yoshiyama, K., Iwase, M., Takeda, M., 2015. Noninvasive prediction of shunt operation outcome in idiopathic normal pressure hydrocephalus. Sci. Rep. 5, 7775. https://doi.org/10.1038/srep07775.

Aoki, Y., Kazui, H., Pascual-Marqui, R.D., Ishii, R., Yoshiyama, K., Kanemoto, H., Suzuki, Y., Sato, S., Azuma, S., Suehiro, T., Matsumoto, T., Hata, M., Canuet, L., Iwase, M., Ikeda, M., 2019. EEG resting-state networks responsible for gait disturbance features in idiopathic normal pressure hydrocephalus. Clin. EEG Neurosci. 50, 210–218. https://doi.org/10.1177/1550059418812156.

Babiloni, C., Binetti, G., Cassetta, E., Forno, G.D., Percio, C.D., Ferreri, F., Ferri, R., Frisoni, G., Hirata, K., Lanuzza, B., Miniussi, C., Moretti, D.V., Nobili, F., Rodriguez, G., Romani, G.L., Salinari, S., Rossini, P.M., 2006. Sources of cortical rhythms change as a function of cognitive impairment in pathological aging: a multicenter study. Clin. Neurophysiol. 117, 252–268. https://doi.org/10.1016/j.clinph.2005.09.019.

Bassett, D.S., Wymbs, N.F., Porter, M.A., Mucha, P.J., Carlson, J.M., Grafton, S.T., 2011. Dynamic reconfiguration of human brain networks during learning. Proc. Natl. Acad. Sci. 108, 7641–7646. https://doi.org/10.1073/pnas.1018985108.

Bassett, D.S., Yang, M., Wymbs, N.F., Grafton, S.T., 2015. Learning-induced autonomy of sensorimotor systems. Nat. Neurosci. 18, 744–751. https://doi.org/10.1038/nn.3993.

Beauchet, O., Annweiler, C., Montero-Odasso, M., Fantino, B., Herrmann, F.R., Allali, G., 2012. Gait control: a specific subdomain of executive function? J. NeuroEngineering Rehabil. 9, 12. https://doi.org/10.1186/1743-0003-9-12.

Beaulieu, C., 2002. The basis of anisotropic water diffusion in the nervous system – a technical review. NMR Biomed. 15, 435–455. https://doi.org/10.1002/nbm.782.

Behrens, T.E.J., Berg, H.J., Jbabdi, S., Rushworth, M.F.S., Woolrich, M.W., 2007. Probabilistic diffusion tractography with multiple fibre orientations: What can we gain? NeuroImage 34, 144–155. https://doi.org/10.1016/j.neuroimage.2006.09.018.

Beissner, F., Meissner, K., Bär, K.-J., Napadow, V., 2013. The autonomic brain: an activation likelihood estimation meta-analysis for central processing of autonomic function. J. Neurosci. 33, 10503–10511. https://doi.org/10.1523/JNEUROSCI.1103-13.2013.

Bihan, D.L., Mangin, J.-F., Poupon, C., Clark, C.A., Pappata, S., Molko, N., Chabriat, H., 2001. Diffusion tensor imaging: concepts and applications. J. Magn. Reson. Imaging 13, 534–546. https://doi.org/10.1002/jmri.1076.

Bohnen, N.I., Jahn, K., 2013. Imaging: what can it tell us about parkinsonian gait? Mov. Disord. 28, 1492–1500. https://doi.org/10.1002/mds.25534.

Boyne, P., Maloney, T., DiFrancesco, M., Fox, M.D., Awosika, O., Aggarwal, P., Woeste, J., Jaroch, L., Braswell, D., Vannest, J., 2018. Resting-state functional connectivity of subcortical locomotor centers explains variance in walking capacity. Hum. Brain Mapp. 39, 4831–4843. https://doi.org/10.1002/hbm.24326.

Braak, H., Ghebremedhin, E., Rüb, U., Bratzke, H., Del Tredici, K., 2004. Stages in the development of Parkinson's disease-related pathology. Cell Tissue Res. 318, 121–134. https://doi.org/10.1007/s00441-004-0956-9.

Calhoun, V.D., Adali, T., 2006. Unmixing fMRI with independent component analysis. IEEE Eng. Med. Biol. Mag. 25, 79–90. https://doi.org/10.1109/MEMB.2006.1607672.

Calhoun, V.D., Miller, R., Pearlson, G., Adalı, T., 2014. The chronnectome: time-varying connectivity networks as the next frontier in fMRI data discovery. Neuron 84, 262–274. https://doi.org/10.1016/j.neuron.2014.10.015.

Cauda, F., D'Agata, F., Sacco, K., Duca, S., Geminiani, G., Vercelli, A., 2011. Functional connectivity of the insula in the resting brain. NeuroImage 55, 8–23. https://doi.org/10.1016/j.neuroimage.2010.11.049.

Chand, G.B., Wu, J., Hajjar, I., Qiu, D., 2017. Interactions of the Salience Network and its subsystems with the default-mode and the central-executive networks in normal aging and mild cognitive impairment. Brain Connect. 7, 401–412. https://doi.org/10.1089/brain.2017.0509.

Chang, L.J., Yarkoni, T., Khaw, M.W., Sanfey, A.G., 2013. Decoding the role of the insula in human cognition: functional parcellation and large-scale reverse inference. Cereb. Cortex 23, 739–749. https://doi.org/10.1093/cercor/bhs065.

Chen, J.E., Chang, C., Greicius, M.D., Glover, G.H., 2015. Introducing co-activation pattern metrics to quantify spontaneous brain network dynamics. NeuroImage 111, 476–488. https://doi.org/10.1016/j.neuroimage.2015.01.057.

Chen, T., Cai, W., Ryali, S., Supekar, K., Menon, V., 2016. Distinct global brain dynamics and spatiotemporal organization of the salience network. PLoS Biol. 14, e1002469. https://doi.org/10.1371/journal.pbio.1002469.

Chen, X., Zhang, H., Zhang, L., Shen, C., Lee, S.-W., Shen, D., 2017. Extraction of dynamic functional connectivity from brain grey matter and white matter for MCI classification. Hum. Brain Mapp. 38, 5019–5034. https://doi.org/10.1002/hbm.23711.

Chistyakov, A.V., Hafner, H., Sinai, A., Kaplan, B., Zaaroor, M., 2012. Motor cortex disinhibition in normal-pressure hydrocephalus: clinical article. J. Neurosurg. 116, 453–459. https://doi.org/10.3171/2011.9.JNS11678.

Daducci, A., Dal Palú, A., Descoteaux, M., Thiran, J.-P., 2016. Microstructure informed tractography: pitfalls and open challenges. Front. Neurosci. 10. https://doi.org/10.3389/fnins.2016.00247.

de Vos, F., Koini, M., Schouten, T.M., Seiler, S., van der Grond, J., Lechner, A., Schmidt, R., de Rooij, M., Rombouts, S.A.R.B., 2018. A comprehensive analysis of resting state fMRI measures to classify individual patients with Alzheimer's disease. NeuroImage 167, 62–72. https://doi.org/10.1016/j.neuroimage.2017.11.025.

Demuru, M., La Cava, S.M., Pani, S.M., Fraschini, M., 2020. A comparison between power spectral density and network metrics: an EEG study. Biomed. Signal Process. Control 57, 101760. https://doi.org/10.1016/j.bspc.2019.101760.

Di Perri, C., Amico, E., Heine, L., Annen, J., Martial, C., Larroque, S.K., Soddu, A., Marinazzo, D., Laureys, S., 2018. Multifaceted Brain Networks Reconfiguration in Disorders of Consciousness Uncovered by Co-Activation Patterns. Human Brain Mapping 39 (1), 89–103.

Diamond, A., 2013. Executive functions. Annu. Rev. Psychol. 64, 135–168. https://doi.org/10.1146/annurev-psych-113011-143750.

Douw, L., van Dellen, E., Gouw, A.A., Griffa, A., de Haan, W., van den Heuvel, M., Hillebrand, A., Van Mieghem, P., Nissen, I.A., Otte, W.M., Reijmer, Y.D., Schoonheim, M.M., Senden, M., van Straaten, E.C.W., Tijms, B.M., Tewarie, P., Stam, C.J., 2019. The road ahead in clinical network neuroscience. Netw. Neurosci. 1–24. https://doi.org/10.1162/netn_a_00103.

Eickhoff, S.B., Laird, A.R., Grefkes, C., Wang, L.E., Zilles, K., Fox, P.T., 2009. Coordinate-based activation likelihood estimation meta-analysis of neuroimaging data: a random-effects approach based on empirical estimates of spatial uncertainty. Hum. Brain Mapp. 30, 2907–2926. https://doi.org/10.1002/hbm.20718.

Eriksen, C.W., Schultz, D.W., 1979. Information processing in visual search: a continuous flow conception and experimental results. Percept. Psychophys. 25, 249–263. https://doi.org/10.3758/BF03198804.

Evans, W.A., 1942. An encephalographic ratio for estimating ventricular enlargement and CEREBRAL ATROPHY. Arch. Neurol. Psychiatry 47, 931–937. https://doi.org/10.1001/archneurpsyc.1942.02290060069004.

Fieremans, E., Jensen, J.H., Helpern, J.A., 2011. White matter characterization with diffusional kurtosis imaging. NeuroImage 58, 177–188. https://doi.org/10.1016/j.neuroimage.2011.06.006.

Fornito, A., Zalesky, A., Breakspear, M., 2015. The connectomics of brain disorders. Nat. Rev. Neurosci. 16, 159–172. https://doi.org/10.1038/nrn3901.
Fox, P.T., Lancaster, J.L., 2002. Mapping context and content: the BrainMap model. Nat. Rev. Neurosci. 3, 319. https://doi.org/10.1038/nrn789.
Fox, P.T., Laird, A.R., Fox, S.P., Fox, P.M., Uecker, A.M., Crank, M., Koenig, S.F., Lancaster, J.L., 2005. Brainmap taxonomy of experimental design: description and evaluation. Hum. Brain Mapp. 25, 185–198. https://doi.org/10.1002/hbm.20141.
Fox, M.D., Corbetta, M., Snyder, A.Z., Vincent, J.L., Raichle, M.E., 2006. Spontaneous neuronal activity distinguishes human dorsal and ventral attention systems. Proc. Natl. Acad. Sci. 103, 10046–10051. https://doi.org/10.1073/pnas.0604187103.
Friston, K.J., 1994. Functional and effective connectivity in neuroimaging: a synthesis. Hum. Brain Mapp. 2, 56–78. https://doi.org/10.1002/hbm.460020107.
Friston, K.J., 2011. Functional and effective connectivity: a review. Brain Connect. 1, 13–36. https://doi.org/10.1089/brain.2011.0008.
Gallia, G.L., Rigamonti, D., Williams, M.A., 2006. The diagnosis and treatment of idiopathic normal pressure hydrocephalus. Nat. Clin. Pract. Neurol. 2, 375. https://doi.org/10.1038/ncpneuro0237.
Gardner, R.C., Boxer, A.L., Trujillo, A., Mirsky, J.B., Guo, C.C., Gennatas, E.D., Heuer, H.W., Fine, E., Zhou, J., Kramer, J.H., Miller, B.L., Seeley, W.W., 2013. Intrinsic connectivity network disruption in progressive supranuclear palsy. Ann. Neurol. 73, 603–616. https://doi.org/10.1002/ana.23844.
Ghaziri, J., Tucholka, A., Girard, G., Houde, J.-C., Boucher, O., Gilbert, G., Descoteaux, M., Lippé, S., Rainville, P., Nguyen, D.K., 2017. The corticocortical structural connectivity of the human insula. Cereb. Cortex 27, 1216–1228. https://doi.org/10.1093/cercor/bhv308.
Giordan, E., Palandri, G., Lanzino, G., Murad, M.H., Elder, B.D., 2018. Outcomes and complications of different surgical treatments for idiopathic normal pressure hydrocephalus: a systematic review and meta-analysis. J. Neurosurg. 1, 1–13. https://doi.org/10.3171/2018.5.JNS1875.
Girard, G., Daducci, A., Petit, L., Thiran, J.-P., Whittingstall, K., Deriche, R., Wassermann, D., Descoteaux, M., 2017. AxTract: toward microstructure informed tractography. Hum. Brain Mapp. 38, 5485–5500. https://doi.org/10.1002/hbm.23741.
Glomb, K., Kringelbach, M.L., Deco, G., Hagmann, P., Pearson, J., Atasoy, S., 2019. Functional harmonics reveal multi-dimensional basis functions underlying cortical organization. bioRxiv 699678. https://doi.org/10.1101/699678.
Greicius, M., 2008. Resting-state functional connectivity in neuropsychiatric disorders. Curr. Opin. Neurol. 21, 424. https://doi.org/10.1097/WCO.0b013e328306f2c5.
Greicius, M.D., Kimmel, D.L., 2012. Neuroimaging insights into network-based neurodegeneration. Curr. Opin. Neurol. 25, 727. https://doi.org/10.1097/WCO.0b013e32835a26b3.
Greicius, M.D., Krasnow, B., Reiss, A.L., Menon, V., 2003. Functional connectivity in the resting brain: a network analysis of the default mode hypothesis. Proc. Natl. Acad. Sci. 100, 253–258. https://doi.org/10.1073/pnas.0135058100.
Griffa, A., Baumann, P.S., Thiran, J.-P., Hagmann, P., 2013. Structural connectomics in brain diseases. NeuroImage 80, 515–526. https://doi.org/10.1016/j.neuroimage.2013.04.056. Mapping the Connectome.
Griffa, A., Ricaud, B., Benzi, K., Bresson, X., Daducci, A., Vandergheynst, P., Thiran, J.-P., Hagmann, P., 2017. Transient networks of spatio-temporal connectivity map communication pathways in brain functional systems. NeuroImage 155, 490–502. https://doi.org/10.1016/j.neuroimage.2017.04.015.
Griffiths, D., 2015. Chapter 7 - functional imaging of structures involved in neural control of the lower urinary tract. In: Vodušek, D.B., Boller, F. (Eds.), Handbook of Clinical Neurology, Neurology of Sexual and Bladder Disorders. Elsevier, pp. 121–133. https://doi.org/10.1016/B978-0-444-63247-0.00007-9.
Gunning-Dixon, F.M., Brickman, A.M., Cheng, J.C., Alexopoulos, G.S., 2009. Aging of cerebral white matter: a review of MRI findings. Int. J. Geriatr. Psychiatry 24, 109–117. https://doi.org/10.1002/gps.2087.
Hagmann, P., 2005. From diffusion MRI to brain connectomics [WWW Document]. Infoscience. https://doi.org/10.5075/epfl-thesis-3230.
Hagmann, P., Jonasson, L., Maeder, P., Thiran, J.-P., Wedeen, V.J., Meuli, R., 2006. Understanding diffusion MR imaging techniques: from scalar diffusion-weighted imaging to diffusion tensor imaging and beyond. RadioGraphics 26, S205–S223. https://doi.org/10.1148/rg.26si065510.
Hakim, S., Adams, R.D., 1965. The special clinical problem of symptomatic hydrocephalus with normal cerebrospinal fluid pressure: Observations on cerebrospinal fluid hydrodynamics. J. Neurol. Sci. 2, 307–327. https://doi.org/10.1016/0022-510X(65)90016-X.
Halperin, J.J., Kurlan, R., Schwalb, J.M., Cusimano, M.D., 2015. Practice Guideline: Idiopathic Normal Pressure Hydrocephalus: Response to Shunting and Predictors of Response 11.
Hari, R., Puce, A., 2017. MEG-EEG Primer. Oxford University Press, Oxford, New York.
Harvie, C., Weissbart, S.J., Kadam-Halani, P., Rao, H., Arya, L.A., 2019. Brain activation during the voiding phase of micturition in healthy adults: a meta-analysis of neuroimaging studies. Clin. Anat. 32, 13–19. https://doi.org/10.1002/ca.23244.
Hattingen, E., Jurcoane, A., Melber, J., Blasel, S., Zanella, F.E., Neumann-Haefelin, T., Singer, O.C., 2010. Diffusion tensor imaging in patients with adult chronic idiopathic hydrocephalus. Neurosurgery 66, 917–924. https://doi.org/10.1227/01.NEU.0000367801.35654.EC.
Hattori, T., Yuasa, T., Aoki, S., Sato, R., Sawaura, H., Mori, T., Mizusawa, H., 2011. Altered microstructure in corticospinal tract in idiopathic normal pressure hydrocephalus: comparison with alzheimer disease and parkinson disease with dementia. Am. J. Neuroradiol. 32, 1681–1687. https://doi.org/10.3174/ajnr.A2570.
Hattori, T., Ito, K., Aoki, S., Yuasa, T., Sato, R., Ishikawa, M., Sawaura, H., Hori, M., Mizusawa, H., 2012a. White matter alteration in idiopathic normal pressure hydrocephalus: tract-based spatial statistics study. Am. J. Neuroradiol. 33, 97–103. https://doi.org/10.3174/ajnr.A2706.
Hattori, T., Sato, R., Aoki, S., Yuasa, T., Mizusawa, H., 2012b. Different patterns of fornix damage in idiopathic normal pressure hydrocephalus and alzheimer disease. Am. J. Neuroradiol. 33, 274–279. https://doi.org/10.3174/ajnr.A2780.
Höglinger, G.U., Respondek, G., Stamelou, M., Kurz, C., Josephs, K.A., Lang, A.E., Mollenhauer, B., Müller, U., Nilsson, C., Whitwell, J.L., Arzberger, T., Englund, E., Gelpi, E., Giese, A., Irwin, D.J., Meissner, W.G., Pantelyat, A., Rajput, A., van Swieten, J.C., Troakes, C., Antonini, A., Bhatia, K.P., Bordelon, Y., Compta, Y., Corvol, J.-C., Colosimo, C., Dickson, D.W., Dodel, R., Ferguson, L., Grossman, M., Kassubek, J., Krismer, F., Levin, J., Lorenzl, S., Morris, H.R., Nestor, P., Oertel, W.H., Poewe, W., Rabinovici, G., Rowe, J.B., Schellenberg, G.D., Seppi, K., van Eimeren, T., Wenning, G.K., Boxer, A.L., Golbe, L.I., Litvan, I., 2017. Clinical diagnosis of progressive supranuclear palsy: the movement disorder society criteria. Mov. Disord. 32, 853–864. https://doi.org/10.1002/mds.26987.
Hoza, D., Vlasák, A., Hořínek, D., Sameš, M., Alfieri, A., 2015. DTI-MRI biomarkers in the search for normal pressure hydrocephalus aetiology: a review. Neurosurg. Rev. 38, 239–244. https://doi.org/10.1007/s10143-014-0584-0.
Huang, W., Bolton, T.A.W., Medaglia, J.D., Bassett, D.S., Ribeiro, A., Ville, D.V.D., 2018. A graph signal processing perspective on functional brain imaging. Proc. IEEE 106, 868–885. https://doi.org/10.1109/JPROC.2018.2798928.
Hugenschmidt, C.E., Burdette, J.H., Morgan, A.R., Williamson, J.D., Kritchevsky, S.B., Laurienti, P.J., 2014. Graph theory analysis of functional brain networks and mobility disability in older adults. J. Gerontol. Ser. A 69, 1399–1406. https://doi.org/10.1093/gerona/glu048.
Hutchison, R.M., Womelsdorf, T., Allen, E.A., Bandettini, P.A., Calhoun, V.D., Corbetta, M., Della Penna, S., Duyn, J.H., Glover, G.H., Gonzalez-Castillo, J., Handwerker, D.A., Keilholz, S., Kiviniemi, V., Leopold, D.A., de Pasquale, F., Sporns, O., Walter, M., Chang, C., 2013. Dynamic functional connectivity: promise, issues, and interpretations. NeuroImage 80, 360–378. https://doi.org/10.1016/j.neuroimage.2013.05.079. Mapping the Connectome.
Ikeda, S., Kazui, H., Tanaka, T., Ishii, R., Aoki, Y., Hata, M., Canuet, L., Yoshiyama, K., Iwase, M., Pascual-Marqui, R., Takeda, M., 2015. Association of cerebrospinal fluid tap-related oscillatory activity and shunt outcome in idiopathic normal-pressure hydrocephalus. Psychogeriatr. Off. J. Jpn. Psychogeriatr. Soc. 15, 191–197. https://doi.org/10.1111/psyg.12106.
Irie, R., Tsuruta, K., Hori, M., Suzuki, M., Kamagata, K., Nakanishi, A., Kamiya, K., Nakajima, M., Miyajima, M., Arai, H., Aoki, S., 2017. Neurite orientation dispersion and density imaging for evaluation of corticospinal tract in idiopathic normal pressure hydrocephalus. J. Radiol. 35, 25–30. https://doi.org/10.1007/s11604-016-0594-7.
Isaacs, A.M., Hamilton, M.G., Williams, M.A., 2019. Idiopathic Normal Pressure Hydrocephalus. In: Limbrick Jr.D.D., Leonard, J.R. (Eds.), Cerebrospinal Fluid Disorders : Lifelong Implications. Springer International Publishing, Cham, pp. 219–235. https://doi.org/10.1007/978-3-319-97928-1_12.
Israelsson, H., Allard, P., Eklund, A., Malm, J., 2016. Symptoms of depression are common in patients with idiopathic normal pressure HydrocephalusThe INPH-CRasH study. Neurosurgery 78, 161–168. https://doi.org/10.1227/NEU.0000000000001093.
Jang, H., Park, S.B., Kim, Y., Kim, K.W., Lee, J.I., Kim, S.T., Lee, K.H., Kang, E.-S., Choe, Y.S., Seo, S.W., Kim, H.J., Kim, Y.J., Yoon, C.W., Na, D.L., 2018. Prognostic value of amyloid PET scan in normal pressure hydrocephalus. J. Neurol. 265, 63–73. https://doi.org/10.1007/s00415-017-8650-5.
Jaraj, D., Rabiei, K., Marlow, T., Jensen, C., Skoog, I., Wikkelsø, C., 2014. Prevalence of idiopathic normal-pressure hydrocephalus. Neurology 82, 1449–1454. https://doi.org/10.1212/WNL.0000000000000342.
Jensen, J.H., Helpern, J.A., 2010. MRI quantification of non-Gaussian water diffusion by kurtosis analysis. NMR Biomed. 23, 698–710. https://doi.org/10.1002/nbm.1518.
Jeppsson, A., Wikkelsö, C., Blennow, K., Zetterberg, H., Constantinescu, R., Remes, A.M., Herukka, S.-K., Rauramaa, T., Nagga, K., Leinonen, V., Tullberg, M., 2019. CSF biomarkers distinguish idiopathic normal pressure hydrocephalus from its mimics. J. Neurol. Neurosurg. https://doi.org/10.1136/jnnp-2019-320826. Psychiatry jnnp-2019-320826.
Jones, D.K., Knösche, T.R., Turner, R., 2013. White matter integrity, fiber count, and other fallacies: the do's and don'ts of diffusion MRI. NeuroImage 73, 239–254. https://doi.org/10.1016/j.neuroimage.2012.06.081.
Jurado, M.B., Rosselli, M., 2007. The elusive nature of executive functions: a review of our current understanding. Neuropsychol. Rev. 17, 213–233. https://doi.org/10.1007/s11065-007-9040-z.
Jurcoane, A., Keil, F., Szelenyi, A., Pfeilschifter, W., Singer, O.C., Hattingen, E., 2014. Directional diffusion of corticospinal tract supports therapy decisions in idiopathic normal-pressure hydrocephalus. Neuroradiology 56, 5–13. https://doi.org/10.1007/s00234-013-1289-8.
Kahya, M., Moon, S., Ranchet, M., Vukas, R.R., Lyons, K.E., Pahwa, R., Akinwuntan, A., Devos, H., 2019. Brain activity during dual task gait and balance in aging and age-related neurodegenerative conditions: a systematic review. Exp. Gerontol. 128, 110756. https://doi.org/10.1016/j.exger.2019.110756.
Kamarajan, C., Pandey, A.K., Chorlian, D.B., Porjesz, B., 2015. The use of current source density as electrophysiological correlates in neuropsychiatric disorders: a review of human studies. Int. J. Psychophysiol. 97, 310–322. https://doi.org/10.1016/j.ijpsycho.2014.10.013. On the benefits of using surface Laplacian (current source density) methodology in electrophysiology.
Kamiya, K., Kamagata, K., Miyajima, M., Nakajima, M., Hori, M., TSURUTA, K., MORI, H., KUNIMATSU, A., ARAI, H., AOKI, S., OHTOMO, K., 2016. Diffusional Kurtosis Imaging in Idiopathic Normal Pressure Hydrocephalus: Correlation with Severity of Cognitive Impairment. Magn. Reson. Med. Sci. 15, 316–323. https://doi.org/10.2463/mrms.mp.2015-0093.
Kamiya, K., Hori, M., Irie, R., Miyajima, M., Nakajima, M., Kamagata, K., Tsuruta, K.,

Saito, A., Nakazawa, M., Suzuki, Y., Mori, H., Kunimatsu, A., Arai, H., Aoki, S., Abe, O., 2017. Diffusion imaging of reversible and irreversible microstructural changes within the corticospinal tract in idiopathic normal pressure hydrocephalus. Neuroimage Clin. 14, 663–671. https://doi.org/10.1016/j.nicl.2017.03.003.

Kang, K., Choi, W., Yoon, U., Lee, J.-M., Lee, H.-W., 2016a. Abnormal white matter integrity in elderly patients with idiopathic normal-pressure hydrocephalus: a tract-based spatial statistics study. Eur. Neurol. 75, 96–103. https://doi.org/10.1159/000443206.

Kang, K., Yoon, U., Choi, W., Lee, H.-W., 2016b. Diffusion tensor imaging of idiopathic normal-pressure hydrocephalus and the cerebrospinal fluid tap test. J. Neurol. Sci. 364, 90–96. https://doi.org/10.1016/j.jns.2016.02.067.

Kanno, S., Saito, M., Kashinoura, T., Nishio, Y., Iizuka, O., Kikuchi, H., Takagi, M., Iwasaki, M., Takahashi, S., Mori, E., 2017. A change in brain white matter after shunt surgery in idiopathic normal pressure hydrocephalus: a tract-based spatial statistics study. Fluids Barriers CNS 14, 1. https://doi.org/10.1186/s12987-016-0048-8.

Karahanoğlu, F.I., Van De Ville, D., 2017. Dynamics of large-scale fMRI networks: deconstruct brain activity to build better models of brain function. Curr. Opin. Biomed. Eng. 3, 28–36. https://doi.org/10.1016/j.cobme.2017.09.008.

Keong, N.C.H., Pena, A., Price, S.J., Czosnyka, M., Czosnyka, Z., Pickard, J.D., 2016. Imaging normal pressure hydrocephalus: theories, techniques, and challenges. Neurosurg. Focus 41, E11. https://doi.org/10.3171/2016.7.FOCUS16194.

Khoo, H.M., Kishima, H., Tani, N., Oshino, S., Maruo, T., Hosomi, K., Yanagisawa, T., Kazui, H., Watanabe, Y., Shimokawa, T., Aso, T., Kawaguchi, A., Yamashita, F., Saitoh, Y., Yoshimine, T., 2016. Default mode network connectivity in patients with idiopathic normal pressure hydrocephalus. J. Neurosurg. 124, 350–358. https://doi.org/10.3171/2015.1.JNS141633.

Kim, H., Park, D.-H., Yi, S., Jeong, E.-J., Yoon, B.C., Czosnyka, M., Sutcliffe, M.P.F., Kim, D.-J., 2015. Finite element analysis for normal pressure hydrocephalus: the effects of the integration of sulci. Med. Image Anal. 24, 235–244. https://doi.org/10.1016/j.media.2015.05.006.

Klassen, B.T., Ahlskog, J.E., 2011. Normal pressure hydrocephalus: how often does the diagnosis hold water? Neurology 77, 1119–1125. https://doi.org/10.1212/WNL.0b013e31822f02f5.

Klinge, P., Hellström, P., Tans, J., Wikkelsø, C., 2012. One-year outcome in the European multicentre study on iNPH. Acta Neurol. Scand. 126, 145–153. https://doi.org/10.1111/j.1600-0404.2012.01676.x.

Kockum, K., Lilja-Lund, O., Larsson, E.-M., Rosell, M., Söderström, L., Virhammar, J., Laurell, K., 2018. The idiopathic normal-pressure hydrocephalus Radscale: a radiological scale for structured evaluation. Eur. J. Neurol. 25, 569–576. https://doi.org/10.1111/ene.13555.

Koechlin, E., Summerfield, C., 2007. An information theoretical approach to prefrontal executive function. Trends Cogn. Sci. (Regul. Ed.) 11, 229–235. https://doi.org/10.1016/j.tics.2007.04.005.

Kouneiher, F., Charron, S., Koechlin, E., 2009. Motivation and cognitive control in the human prefrontal cortex. Nat. Neurosci. 12, 939–945. https://doi.org/10.1038/nn.2321.

Koyama, T., Marumoto, K., Domen, K., Miyake, H., 2013. White matter characteristics of idiopathic normal pressure hydrocephalus: a diffusion tensor tract-based spatial statistic study. Neurol. Med. Chir. (Tokyo) 53, 601–608.

Krishnan, A., Williams, L.J., McIntosh, A.R., Abdi, H., 2011. Partial Least Squares (PLS) methods for neuroimaging: a tutorial and review. NeuroImage 56, 455–475. https://doi.org/10.1016/j.neuroimage.2010.07.034. Multivariate Decoding and Brain Reading.

Kubo, Y., Kazui, H., Yoshida, T., Kito, Y., Kimura, N., Tokunaga, H., Ogino, A., Miyake, H., Ishikawa, M., Takeda, M., 2008. Validation of grading scale for evaluating symptoms of idiopathic normal-pressure hydrocephalus. Dement. Geriatr. Cogn. Disord. 25, 37–45. https://doi.org/10.1159/000111149.

Kurth, F., Zilles, K., Fox, P.T., Laird, A.R., Eickhoff, S.B., 2010. A link between the systems: functional differentiation and integration within the human insula revealed by meta-analysis. Brain Struct. Funct. 214, 519–534. https://doi.org/10.1007/s00429-010-0255-z.

Lancaster, J.L., Woldorff, M.G., Parsons, L.M., Liotti, M., Freitas, C.S., Rainey, L., Kochunov, P.V., Nickerson, D., Mikiten, S.A., Fox, P.T., 2000. Automated Talairach Atlas labels for functional brain mapping. Hum. Brain Mapp. 10, 120–131. https://doi.org/10.1002/1097-0193(200007)10:3<120::AID-HBM30>3.0.CO;2-8.

Lancaster, J.L., Tordesillas-Gutiérrez, D., Martinez, M., Salinas, F., Evans, A., Zilles, K., Mazziotta, J.C., Fox, P.T., 2007. Bias between MNI and Talairach coordinates analyzed using the ICBM-152 brain template. Hum. Brain Mapp. 28, 1194–1205. https://doi.org/10.1002/hbm.20345.

Lenfeldt, N., Larsson, A., Nyberg, L., Andersson, M., Birgander, R., Eklund, A., Malm, J., 2008. Idiopathic normal pressure hydrocephalus: increased supplementary motor activity accounts for improvement after CSF drainage. Brain 131, 2904–2912. https://doi.org/10.1093/brain/awn232.

Li, Q., Yang, G., Li, Z., Qi, Y., Cole, M.W., Liu, X., 2017. Conflict detection and resolution rely on a combination of common and distinct cognitive control networks. Neurosci. Biobehav. Rev. 83, 123–131. https://doi.org/10.1016/j.neubiorev.2017.09.032.

Li, K.Z.H., Bherer, L., Mirelman, A., Maidan, I., Hausdorff, J.M., 2018. Cognitive involvement in balance, gait and dual-tasking in aging: a focused review from a neuroscience of aging perspective. Front. Neurol. 9. https://doi.org/10.3389/fneur.2018.00913.

Liu, X., Duyn, J.H., 2013. Time-varying functional network information extracted from brief instances of spontaneous brain activity. Proc. Natl. Acad. Sci. 110, 4392–4397. https://doi.org/10.1073/pnas.1216856110.

Luikku, A.J., Hall, A., Nerg, O., Koivisto, A.M., Hiltunen, M., Helisalmi, S., Herukka, S.-K., Sutela, A., Kojoukhova, M., Mattila, J., Lötjönen, J., Rummukainen, J., Alafuzoff, I., Jääskeläinen, J.E., Remes, A.M., Soininen, H., Leinonen, V., 2016. Multimodal analysis to predict shunt surgery outcome of 284 patients with suspected idiopathic normal pressure hydrocephalus. Acta Neurochir. (Wien) 158, 2311–2319. https://doi.org/10.1007/s00701-016-2980-4.

Lustig, C., Snyder, A.Z., Bhakta, M., O'Brien, K.C., McAvoy, M., Raichle, M.E., Morris, J.C., Buckner, R.L., 2003. Functional deactivations: change with age and dementia of the Alzheimer type. Proc. Natl. Acad. Sci. 100, 14504–14509. https://doi.org/10.1073/pnas.2235925100.

Magdalinou, N.K., Ling, H., Smith, J.D.S., Schott, J.M., Watkins, L.D., Lees, A.J., 2013. Normal pressure hydrocephalus or progressive supranuclear palsy? A clinicopathological case series. J. Neurol. 260, 1009–1013. https://doi.org/10.1007/s00415-012-6745-6.

Maidan, I., Jacob, Y., Giladi, N., Hausdorff, J.M., Mirelman, A., 2019. Altered organization of the dorsal attention network is associated with freezing of gait in Parkinson's disease. Parkinsonism Relat. Disord. 63, 77–82. https://doi.org/10.1016/j.parkreldis.2019.02.036.

Malm, J., Graff-Radford, N.R., Ishikawa, M., Kristensen, B., Leinonen, V., Mori, E., Owler, B.K., Tullberg, M., Williams, M.A., Relkin, N.R., 2013a. Influence of comorbidities in idiopathic normal pressure hydrocephalus — research and clinical care. A report of the ISHCSF task force on comorbidities in INPH. Fluids Barriers CNS 10, 22. https://doi.org/10.1186/2045-8118-10-22.

Malm, J., Graff-Radford, N.R., Ishikawa, M., Kristensen, B., Leinonen, V., Mori, E., Owler, B.K., Tullberg, M., Williams, M.A., Relkin, N.R., 2013b. Influence of comorbidities in idiopathic normal pressure hydrocephalus — research and clinical care. A report of the ISHCSF task force on comorbidities in INPH. Fluids Barriers CNS 10, 22. https://doi.org/10.1186/2045-8118-10-22.

Manniche, C., Hejl, A.-M., Hasselbalch, S.G., Simonsen, A.H., 2019. Cerebrospinal Fluid Biomarkers in Idiopathic Normal Pressure Hydrocephalus versus Alzheimer's Disease and Subcortical Ischemic Vascular Disease: A Systematic Review. J. Alzheimers Dis. 68, 267–279. https://doi.org/10.3233/JAD-180816.

Marmarou, A., Bergsneider, M., Klinge, P., Relkin, N., Black, P.M., 2005. The value of supplemental prognostic tests for the preoperative assessment of idiopathic normal-pressure hydrocephalus. Neurosurgery 57https://doi.org/10.1227/01.NEU.0000168184.01002.60. S2-17-S2-28.

Marumoto, K., Koyama, T., Hosomi, M., Kodama, N., Miyake, H., Domen, K., 2012. Diffusion tensor imaging in elderly patients with idiopathic normal pressure hydrocephalus or Parkinson's disease: diagnosis of gait abnormalities. Fluids Barriers CNS 9, 20. https://doi.org/10.1186/2045-8118-9-20.

Menon, V., 2015. Salience network. Brain Mapping. Elsevier, pp. 597–611. https://doi.org/10.1016/B978-0-12-397025-1.00052-X.

Meskaldji, D.-E., Preti, M.G., Bolton, T., Montandon, M.-L., Rodriguez, C., Morgenthaler, A.S., Giannakopoulos, P., Haller, S., Van De Ville, D., 2016. Predicting individual scores from resting state fMRI using partial least squares regression, in: 2016 IEEE 13th International symposium on biomedical imaging (ISBI). In: Presented at the 2016 IEEE 13th International Symposium on Biomedical Imaging (ISBI 2016). IEEE, Prague, Czech Republic. pp. 1311–1314. https://doi.org/10.1109/ISBI.2016.7493508.

Mirelman, A., Maidan, I., Bernad-Elazari, H., Shustack, S., Giladi, N., Hausdorff, J.M., 2017. Effects of aging on prefrontal brain activation during challenging walking conditions. Brain Cogn. 115, 41–46. https://doi.org/10.1016/j.bandc.2017.04.002.

Mito, R., Raffelt, D., Dhollander, T., Vaughan, D.N., Tournier, J.-D., Salvado, O., Brodtmann, A., Rowe, C.C., Villemagne, V.L., Connelly, A., 2018. Fibre-specific white matter reductions in Alzheimer's disease and mild cognitive impairment. Brain 141, 888–902. https://doi.org/10.1093/brain/awx355.

Miyoshi, N., Kazui, H., Ogino, A., Ishikawa, M., Miyake, H., Tokunaga, H., Ikejiri, Y., Takeda, M., 2005. Association between cognitive impairment and gait disturbance in patients with idiopathic normal pressure hydrocephalus. Dement. Geriatr. Cogn. Disord. 20, 71–76. https://doi.org/10.1159/000085858.

Moher, D., Liberati, A., Tetzlaff, J., Altman, D.G., Group, T.P., 2009. Preferred reporting items for systematic reviews and meta-analyses: the PRISMA statement. PLoS Med. 6, e1000097. https://doi.org/10.1371/journal.pmed.1000097.

Mori, E., Ishikawa, M., Kato, T., Kazui, H., Miyake, H., Miyajima, M., Nakajima, M., Hashimoto, M., Kuriyama, N., Tokuda, T., Ishii, K., Kaijima, M., Hirata, Y., Saito, M., Arai, H., 2012. Guidelines for management of idiopathic normal pressure hydrocephalus: second edition. Neurol. Med. Chir. (Tokyo) 52, 775–809. https://doi.org/10.2176/nmc.52.775.

Morris, R., Lord, S., Bunce, J., Burn, D., Rochester, L., 2016. Gait and cognition: mapping the global and discrete relationships in ageing and neurodegenerative disease. Neurosci. Biobehav. Rev. 64, 326–345. https://doi.org/10.1016/j.neubiorev.2016.02.012.

Nakanishi, A., Fukunaga, I., Hori, M., Masutani, Y., Takaaki, H., Miyajima, M., Aoki, S., 2013. Microstructural changes of the corticospinal tract in idiopathic normal pressure hydrocephalus: a comparison of diffusion tensor and diffusional kurtosis imaging. Neuroradiology 55, 971–976. https://doi.org/10.1007/s00234-013-1201-6.

Nardone, R., Golaszewski, S., Schwenker, K., Brigo, F., Maccarrone, M., Versace, V., Sebastianelli, L., Saltuari, L., Höller, Y., 2019. Cholinergic transmission is impaired in patients with idiopathic normal-pressure hydrocephalus: a TMS study. J. Neural Transm. https://doi.org/10.1007/s00702-019-02036-6.

Nickerson, L.D., Smith, S.M., Öngür, D., Beckmann, C.F., 2017. Using dual regression to investigate network shape and amplitude in functional connectivity analyses. Front. Neurosci. 11. https://doi.org/10.3389/fnins.2017.00115.

O'Donnell, L.J., Westin, C.-F., Golby, A.J., 2009. Tract-based morphometry for white matter group analysis. NeuroImage 45, 832–844. https://doi.org/10.1016/j.neuroimage.2008.12.023.

Ogata, Y., Ozaki, A., Ota, M., Oka, Y., Nishida, N., Tabu, H., Sato, N., Hanakawa, T., 2017. Interhemispheric resting-state functional connectivity predicts severity of idiopathic normal pressure hydrocephalus. Front. Neurosci. 11. https://doi.org/10.3389/fnins.

2017.00470.
Ossenkoppele, R., Iaccarino, L., Schonhaut, D.R., Brown, J.A., La Joie, R., O'Neil, J.P., Janabi, M., Baker, S.L., Kramer, J.H., Gorno-Tempini, M.-L., Miller, B.L., Rosen, H.J., Seeley, W.W., Jagust, W.J., Rabinovici, G.D., 2019. Tau covariance patterns in Alzheimer's disease patients match intrinsic connectivity networks in the healthy brain. Neuroimage Clin. 23, 101848. https://doi.org/10.1016/j.nicl.2019.101848.
Pagonabarraga, J., Kulisevsky, J., Strafella, A.P., Krack, P., 2015. Apathy in Parkinson's disease: clinical features, neural substrates, diagnosis, and treatment. Lancet Neurol. 14, 518–531. https://doi.org/10.1016/S1474-4422(15)00019-8.
Palmqvist, S., Schöll, M., Strandberg, O., Mattsson, N., Stomrud, E., Zetterberg, H., Blennow, K., Landau, S., Jagust, W., Hansson, O., 2017. Earliest accumulation of β-amyloid occurs within the default-mode network and concurrently affects brain connectivity. Nat. Commun. 8, 1–13. https://doi.org/10.1038/s41467-017-01150-x.
Panagiotaki, E., Schneider, T., Siow, B., Hall, M.G., Lythgoe, M.F., Alexander, D.C., 2012. Compartment models of the diffusion MR signal in brain white matter: a taxonomy and comparison. NeuroImage 59, 2241–2254. https://doi.org/10.1016/j.neuroimage.2011.09.081.
Park, D.C., Reuter-Lorenz, P., 2009. The adaptive brain: aging and neurocognitive scaffolding. Annu. Rev. Psychol. 60, 173–196. https://doi.org/10.1146/annurev.psych.59.103006.093656.
Pascual-Leone, A., Walsh, V., Rothwell, J., 2000. Transcranial magnetic stimulation in cognitive neuroscience – virtual lesion, chronometry, and functional connectivity. Curr. Opin. Neurobiol. 10, 232–237. https://doi.org/10.1016/S0959-4388(00)00081-7.
Pasternak, O., Sochen, N., Gur, Y., Intrator, N., Assaf, Y., 2009. Free water elimination and mapping from diffusion MRI. Magn. Reson. Med. 62, 717–730. https://doi.org/10.1002/mrm.22055.
Peña, A., Harris, N.G., Bolton, M.D., Czosnyka, M., Pickard, J.D., 2002. Communicating hydrocephalus: the biomechanics of progressive ventricular enlargement revisited. In: Czosnyka, M., Pickard, J.D., Kirkpatrick, P.J., Smielewski, P., Hutchinson, P. (Eds.), Intracranial Pressure and Brain Biochemical Monitoring, Acta Neurochirurgica Supplements. Springer, Vienna, pp. 59–63.
Peterson, K.A., Housden, C.R., Killikelly, C., DeVito, E.E., Keong, N.C., Savulich, G., Czosnyka, Z., Pickard, J.D., Sahakian, B.J., 2016. Apathy, ventriculomegaly and neurocognitive improvement following shunt surgery in normal pressure hydrocephalus. Br. J. Neurosurg. 30, 38–42. https://doi.org/10.3109/02688697.2015.1029429.
Petrovic, M., Bolton, T.A.W., Preti, M.G., Liégeois, R., Van De Ville, D., 2019. Guided graph spectral embedding: application to the C. Elegans connectome. Netw. Neurosci. 3, 807–826. https://doi.org/10.1162/netn_a_00084.
Picascia, M., Zangaglia, R., Bernini, S., Minafra, B., Sinforiani, E., Pacchetti, C., 2016. A review of cognitive impairment and differential diagnosis in idiopathic normal pressure hydrocephalus. Funct. Neurol. 30, 217–228. https://doi.org/10.11138/FNeur/2015.30.4.217.
Pievani, M., Filippini, N., van den Heuvel, M.P., Cappa, S.F., Frisoni, G.B., 2014. Brain connectivity in neurodegenerative diseases—from phenotype to proteinopathy. Nat. Rev. Neurol. 10, 620–633. https://doi.org/10.1038/nrneurol.2014.178.
Pomeraniec, I.J., Bond, A.E., Lopes, M.B., Jane, J.A., 2016. Concurrent Alzheimer's pathology in patients with clinical normal pressure hydrocephalus: correlation of high-volume lumbar puncture results, cortical brain biopsies, and outcomes. J. Neurosurg. 124, 382–388. https://doi.org/10.3171/2015.2.JNS142318.
Preti, M.G., Ville, D.V.D., 2019. Decoupling of brain function from structure reveals regional behavioral specialization in humans. Nat. Commun. 10, 1–7. https://doi.org/10.1038/s41467-019-12765-7.
Preti, M.G., Bolton, T.A., Van De Ville, D., 2017. The dynamic functional connectome: state-of-the-art and perspectives. NeuroImage 160, 41–54. https://doi.org/10.1016/j.neuroimage.2016.12.061. Functional Architecture of the Brain.
Pyykkö, O.T., Nerg, O., Niskasaari, H.-M., Niskasaari, T., Koivisto, A.M., Hiltunen, M., Pihlajamäki, J., Rauramaa, T., Kojoukhova, M., Alafuzoff, I., Soininen, H., Jääskeläinen, J.E., Leinonen, V., 2018. Incidence, comorbidities, and mortality in idiopathic normal pressure hydrocephalus. World Neurosurg. 112, e624–e631. https://doi.org/10.1016/j.wneu.2018.01.107.
Quevenco, F.C., Preti, M.G., van Bergen, J.M.G., Hua, J., Wyss, M., Li, X., Schreiner, S.J., Steininger, S.C., Meyer, R., Meier, I.B., Brickman, A.M., Leh, S.E., Gietl, A.F., Buck, A., Nitsch, R.M., Pruessmann, K.P., van Zijl, P.C.M., Hock, C., Van De Ville, D., Unschuld, P.G., 2017. Memory performance-related dynamic brain connectivity indicates pathological burden and genetic risk for Alzheimer's disease. Alzheimers Res. Ther. 9, 24. https://doi.org/10.1186/s13195-017-0249-7.
Raffelt, D.A., Tournier, J.-D., Smith, R.E., Vaughan, D.N., Jackson, G., Ridgway, G.R., Connelly, A., 2017. Investigating white matter fibre density and morphology using fixel-based analysis. NeuroImage 144, 58–73. https://doi.org/10.1016/j.neuroimage.2016.09.029.
Raichle, M.E., 2015. The brain's default mode network. Annu. Rev. Neurosci. 38, 433–447. https://doi.org/10.1146/annurev-neuro-071013-014030.
Raj, A., Kuceyeski, A., Weiner, M., 2012. A network diffusion model of disease progression in dementia. Neuron 73, 1204–1215. https://doi.org/10.1016/j.neuron.2011.12.040.
Relkin, N., Marmarou, A., Klinge, P., Bergsneider, M., Black, P.M., 2005. Diagnosing idiopathic normal-pressure hydrocephalus. Neurosurgery 57https://doi.org/10.1227/01.NEU.0000168185.29659.C5. S2-4-S2-16.
Richiardi, J., Eryilmaz, H., Schwartz, S., Vuilleumier, P., Van De Ville, D., 2011. Decoding brain states from fMRI connectivity graphs. NeuroImage 56, 616–626. https://doi.org/10.1016/j.neuroimage.2010.05.081. Multivariate Decoding and Brain Reading.
Richiardi, J., Achard, S., Bunke, H., Ville, D.V.D., 2013. Machine learning with brain graphs: predictive modeling approaches for functional imaging in systems neuroscience. IEEE Signal Process. Mag. 30, 58–70. https://doi.org/10.1109/MSP.2012.2233865.
Rothwell, J.C., Day, B.L., Thompson, P.D., Kujirai, T., 2009. Short latency intracortical inhibition: one of the most popular tools in human motor neurophysiology. J. Physiol. (Paris) 587, 11–12. https://doi.org/10.1113/jphysiol.2008.162461.
Saito, M., Nishio, Y., Kanno, S., Uchiyama, M., Hayashi, A., Takagi, M., Kikuchi, H., Yamasaki, H., Shimomura, T., Iizuka, O., Mori, E., 2011. Cognitive profile of idiopathic normal pressure hydrocephalus. Dement. Geriatr. Cogn. Disord. Extra 1, 202–211. https://doi.org/10.1159/000328924.
Saito, A., Kamagata, K., Ueda, R., Nakazawa, M., Andica, C., Irie, R., Nakajima, M., Miyajima, M., Hori, M., Tanaka, F., Arai, H., Aoki, S., 2019. Ventricular volumetry and free-water corrected diffusion tensor imaging of the anterior thalamic radiation in idiopathic normal pressure hydrocephalus. J. Neuroradiol. https://doi.org/10.1016/j.neurad.2019.04.003.
Sand, T., Bovim, G., Gimse, R., 1994. Quantitative electroencephalography in idiopathic normal pressure hydrocephalus: relationship to CSF outflow resistance and the CSF tap-test. Acta Neurol. Scand. 89, 317–322. https://doi.org/10.1111/j.1600-0404.1994.tb02641.x.
Scala, G.D., Dupuy, M., Guillaud, E., Doat, E., Barse, E., Dillhareguy, B., Jean, F.A.M., Audiffren, M., Cazalets, J.R., Chanraud, S., 2019. Efficiency of sensorimotor networks: posture and gait in young and older adults. Exp. Aging Res. 45, 41–56. https://doi.org/10.1080/0361073X.2018.1560108.
Schmierer, K., Scaravilli, F., Altmann, D.R., Barker, G.J., Miller, D.H., 2004. Magnetization transfer ratio and myelin in postmortem multiple sclerosis brain. Ann. Neurol. 56, 407–415. https://doi.org/10.1002/ana.20202.
Seeley, W.W., Menon, V., Schatzberg, A.F., Keller, J., Glover, G.H., Kenna, H., Reiss, A.L., Greicius, M.D., 2007. Dissociable intrinsic connectivity networks for salience processing and executive control. J. Neurosci. 27, 2349–2356. https://doi.org/10.1523/JNEUROSCI.5587-06.2007.
Seeley, W.W., Crawford, R.K., Zhou, J., Miller, B.L., Greicius, M.D., 2009. Neurodegenerative diseases target large-scale human brain networks. Neuron 62, 42–52. https://doi.org/10.1016/j.neuron.2009.03.024.
Seidler, R.D., Bernard, J.A., Burutolu, T.B., Fling, B.W., Gordon, M.T., Gwin, J.T., Kwak, Y., Lipps, D.B., 2010. Motor control and aging: links to age-related brain structural, functional, and biochemical effects. Neurosci. Biobehav. Rev. 34, 721–733. https://doi.org/10.1016/j.neubiorev.2009.10.005. Special Section: Dopaminergic Modulation of Lifespan Cognition.
Seidlitz, J., Váša, F., Shinn, M., Romero-Garcia, R., Whitaker, K.J., Vértes, P.E., Wagstyl, K., Kirkpatrick Reardon, P., Clasen, L., Liu, S., Messinger, A., Leopold, D.A., Fonagy, P., Dolan, R.J., Jones, P.B., Goodyer, I.M., Raznahan, A., Bullmore, E.T., 2018. Morphometric similarity networks detect microscale cortical organization and predict inter-individual cognitive variation. Neuron 97 (231–247), e7. https://doi.org/10.1016/j.neuron.2017.11.039.
Selge, C., Schoeberl, F., Zwergal, A., Nuebling, G., Brandt, T., Dieterich, M., Schniepp, R., Jahn, K., 2018. Gait analysis in PSP and NPH: dual-task conditions make the difference. Neurology 90, e1021–e1028. https://doi.org/10.1212/WNL.0000000000005168.
Seo, J.-G., Kang, K., Jung, J.-Y., Park, S.-P., Lee, M.-G., Lee, H.-W., 2014. Idiopathic normal pressure hydrocephalus, quantitative EEG findings, and the cerebrospinal fluid tap test: a pilot study. J. Clin. Neurophysiol. 31, 594. https://doi.org/10.1097/WNP.0000000000000105.
Shaw, R., Mahant, N., Jacobson, E., Owler, B., 2016. A review of clinical outcomes for gait and other variables in the surgical treatment of idiopathic normal pressure hydrocephalus. Mov. Disord. Clin. Pract. 3, 331–341. https://doi.org/10.1002/mdc3.12335.
Shuman, D.I., Narang, S.K., Frossard, P., Ortega, A., Vandergheynst, P., 2013. The emerging field of signal processing on graphs: extending high-dimensional data analysis to networks and other irregular domains. IEEE Signal Process. Mag. 30, 83–98. https://doi.org/10.1109/MSP.2012.2235192.
Shuman, D.I., Ricaud, B., Vandergheynst, P., 2016. Vertex-frequency analysis on graphs. Appl. Comput. Harmon. Anal. 40, 260–291. https://doi.org/10.1016/j.acha.2015.02.005.
Siasios, I., Kapsalaki, E.Z., Fountas, K.N., Fotiadou, A., Dorsch, A., Vakharia, K., Pollina, J., Dimopoulos, V., 2016. The role of diffusion tensor imaging and fractional anisotropy in the evaluation of patients with idiopathic normal pressure hydrocephalus: a literature review. Neurosurg. Focus 41, E12. https://doi.org/10.3171/2016.6.FOCUS16192.
Smith, S.M., Jenkinson, M., Johansen-Berg, H., Rueckert, D., Nichols, T.E., Mackay, C.E., Watkins, K.E., Ciccarelli, O., Cader, M.Z., Matthews, P.M., Behrens, T.E.J., 2006. Tract-based spatial statistics: voxelwise analysis of multi-subject diffusion data. NeuroImage 31, 1487–1505. https://doi.org/10.1016/j.neuroimage.2006.02.024.
Sperling, R.A., LaViolette, P.S., O'Keefe, K., O'Brien, J., Rentz, D.M., Pihlajamaki, M., Marshall, G., Hyman, B.T., Selkoe, D.J., Hedden, T., Buckner, R.L., Becker, J.A., Johnson, K.A., 2009. Amyloid Deposition Is Associated with Impaired Default Network Function in Older Persons without Dementia. Neuron 63, 178–188. https://doi.org/10.1016/j.neuron.2009.07.003.
Sporns, O., Tononi, G., Kötter, R., 2005. The human connectome: a structural description of the human brain. PLoS Comput. Biol. 1, e42. https://doi.org/10.1371/journal.pcbi.0010042.
Sridharan, D., Levitin, D.J., Menon, V., 2008. A critical role for the right fronto-insular cortex in switching between central-executive and default-mode networks. Proc. Natl. Acad. Sci. 105, 12569–12574. https://doi.org/10.1073/pnas.0800005105.
Stam, C.J., 2014. Modern network science of neurological disorders. Nat. Rev. Neurosci. 15, 683–695. https://doi.org/10.1038/nrn3801.
Stam, C.J., Jones, B.F., Nolte, G., Breakspear, M., Scheltens, P., 2007. Small-world networks and functional connectivity in alzheimer's disease. Cereb. Cortex 17, 92–99. https://doi.org/10.1093/cercor/bhj127.

Stolze, H., Kuhtz-Buschbeck, J.P., Drücke, H., Jöhnk, K., Illert, M., Deuschl, G., 2001. Comparative analysis of the gait disorder of normal pressure hydrocephalus and Parkinson's disease. J. Neurol. Neurosurg. Psychiatry 70, 289–297. https://doi.org/10.1136/jnnp.70.3.289.

Tagliazucchi, E., Von Wegner, F., Morzelewski, A., Brodbeck, V., Laufs, H., 2012. Dynamic BOLD functional connectivity in humans and its electrophysiological correlates. Front. Hum. Neurosci. 6. https://doi.org/10.3389/fnhum.2012.00339.

Takakusaki, K., 2013. Neurophysiology of gait: from the spinal cord to the frontal lobe. Mov. Disord. 28, 1483–1491. https://doi.org/10.1002/mds.25669.

Takakusaki, K., 2017. Functional neuroanatomy for posture and gait control. J. Mov. Disord. 10, 1–17. https://doi.org/10.14802/jmd.16062.

Tarnaris, A., Kitchen, N.D., Watkins, L.D., 2009. Noninvasive biomarkers in normal pressure hydrocephalus: evidence for the role of neuroimaging: a review. J. Neurosurg. 110, 837–851. https://doi.org/10.3171/2007.9.17572.

Tewarie, P., Liuzzi, L., O'Neill, G.C., Quinn, A.J., Griffa, A., Woolrich, M.W., Stam, C.J., Hillebrand, A., Brookes, M.J., 2019. Tracking dynamic brain networks using high temporal resolution MEG measures of functional connectivity. NeuroImage 200, 38–50. https://doi.org/10.1016/j.neuroimage.2019.06.006.

Toma, A.K., Papadopoulos, M.C., Stapleton, S., Kitchen, N.D., Watkins, L.D., 2013. Systematic review of the outcome of shunt surgery in idiopathic normal-pressure hydrocephalus. Acta Neurochir. (Wien) 155, 1977–1980. https://doi.org/10.1007/s00701-013-1835-5.

Tomasi, D., Volkow, N.D., 2012. Aging and functional brain networks. Mol. Psychiatry 17, 549–558. https://doi.org/10.1038/mp.2011.81.

Tournier, J.-D., Mori, S., Leemans, A., 2011. Diffusion tensor imaging and beyond. Magn. Reson. Med. 65, 1532–1556. https://doi.org/10.1002/mrm.22924.

Turkeltaub, P.E., Eden, G.F., Jones, K.M., Zeffiro, T.A., 2002. Meta-analysis of the functional neuroanatomy of single-word reading: method and validation. NeuroImage 16, 765–780. https://doi.org/10.1006/nimg.2002.1131.

Turkeltaub, P.E., Eickhoff, S.B., Laird, A.R., Fox, M., Wiener, M., Fox, P., 2012. Minimizing within-experiment and within-group effects in activation likelihood estimation meta-analyses. Hum. Brain Mapp. 33, 1–13. https://doi.org/10.1002/hbm.21186.

Uddin, L.Q., 2015. Salience processing and insular cortical function and dysfunction. Nat. Rev. Neurosci. 16, 55–61. https://doi.org/10.1038/nrn3857.

Uddin, L.Q., Nomi, J.S., Hebert-Seropian, B., Ghaziri, J., Boucher, O., 2017. Structure and function of the human insula. J. Clin. Neurophysiol. Off. Publ. Am. Electroencephalogr. Soc. 34, 300–306. https://doi.org/10.1097/WNP.0000000000000377.

Valkanova, V., Ebmeier, K.P., 2017. What can gait tell us about dementia? Review of epidemiological and neuropsychological evidence. Gait Posture 53, 215–223. https://doi.org/10.1016/j.gaitpost.2017.01.024.

van den Heuvel, M.P., Hulshoff Pol, H.E., 2010. Exploring the brain network: a review on resting-state fMRI functional connectivity. Eur. Neuropsychopharmacol. 20, 519–534. https://doi.org/10.1016/j.euroneuro.2010.03.008.

Van Der Meulen, M., Allali, G., Rieger, S.W., Assal, F., Vuilleumier, P., 2014. The influence of individual motor imagery ability on cerebral recruitment during gait imagery. Hum. Brain Mapp. 35, 455–470. https://doi.org/10.1002/hbm.22192.

van Veen, V., Carter, C.S., 2002. The anterior cingulate as a conflict monitor: fMRI and ERP studies. Physiol. Behav. 77, 477–482. https://doi.org/10.1016/S0031-9384(02)00930-7.

Verghese, J., Wang, C., Lipton, R.B., Holtzer, R., 2013. Motoric cognitive risk syndrome and the risk of dementia. J. Gerontol. Ser. A 68, 412–418. https://doi.org/10.1093/gerona/gls191.

Vossel, S., Geng, J.J., Fink, G.R., 2014. Dorsal and ventral attention systems. Neuroscientist 20, 150–159. https://doi.org/10.1177/1073858413494269.

Vucic, S., Kiernan, M.C., 2017. Transcranial magnetic stimulation for the assessment of neurodegenerative disease. Neurotherapeutics 14, 91–106. https://doi.org/10.1007/s13311-016-0487-6.

Wallenstein, M.B., McKhann, G.M., 2010. Salomón Hakim and the discovery of normal-pressure hydrocephalus. Neurosurgery 67, 155–159. https://doi.org/10.1227/01.NEU.0000370058.12120.0E.

Whitwell, J.L., Avula, R., Master, A., Vemuri, P., Senjem, M.L., Jones, D.T., Jack, C.R., Josephs, K.A., 2011a. Disrupted thalamocortical connectivity in PSP: a resting-state fMRI, DTI, and VBM study. Parkinsonism Relat. Disord. 17, 599–605. https://doi.org/10.1016/j.parkreldis.2011.05.013.

Whitwell, J.L., Master, A.V., Avula, R., Kantarci, K., Eggers, S.D., Edmonson, H.A., Jack, C.R., Josephs, K.A., 2011b. Clinical correlates of white matter tract degeneration in progressive supranuclear palsy. Arch. Neurol. 68, 753–760. https://doi.org/10.1001/archneurol.2011.107.

Wikkelsø, C., Hellström, P., Klinge, P.M., Tans, J.T.J., Group, on behalf of the E. iNPH M.S, 2013. The European iNPH Multicentre Study on the predictive values of resistance to CSF outflow and the CSF Tap Test in patients with idiopathic normal pressure hydrocephalus. J. Neurol. Neurosurg. Psychiatry 84, 562–568. https://doi.org/10.1136/jnnp-2012-303314.

Williams, M.A., Malm, J., 2016. Diagnosis and treatment of idiopathic normal pressure hydrocephalus. Contin. Lifelong Learn. Neurol. 22, 579–599. https://doi.org/10.1212/CON.0000000000000305.

Winston, G.P., 2012. The physical and biological basis of quantitative parameters derived from diffusion MRI. Quant. Imaging Med. Surg. 2, 254–265. https://doi.org/10.3978/j.issn.2223-4292.2012.12.05.

Xia, C.H., Ma, Z., Ciric, R., Gu, S., Betzel, R.F., Kaczkurkin, A.N., Calkins, M.E., Cook, P.A., de la Garza, A.G., Vandekar, S.N., Cui, Z., Moore, T.M., Roalf, D.R., Ruparel, K., Wolf, D.H., Davatzikos, C., Gur, R.C., Gur, R.E., Shinohara, R.T., Bassett, D.S., Satterthwaite, T.D., 2018. Linked dimensions of psychopathology and connectivity in functional brain networks. Nat. Commun. 9, 1–14. https://doi.org/10.1038/s41467-018-05317-y.

Yakovlev, P.I., 1947. Paraplegias of hydrocephalics; a clinical note and interpretation. American journal of mental deficiency 51 (4), 561–576.

Yarkoni, T., Poldrack, R.A., Nichols, T.E., Van Essen, D.C., Wager, T.D., 2011. Large-scale automated synthesis of human functional neuroimaging data. Nat. Methods 8, 665–670. https://doi.org/10.1038/nmeth.1635.

Yin, L.-K., Zheng, J.-J., Tian, J.-Q., Hao, X.-Z., Li, C.-C., Ye, J.-D., Zhang, Y.-X., Yu, H., Yang, Y.-M., 2018. Abnormal gray matter structural networks in idiopathic normal pressure hydrocephalus. Front. Aging Neurosci. 10. https://doi.org/10.3389/fnagi.2018.00356.

Younes, K., Hasan, K.M., Kamali, A., McGough, C.E., Keser, Z., Hasan, O., Melicher, T., Kramer, L.A., Schulz, P.E., 2019. Diffusion tensor imaging of the superior thalamic radiation and cerebrospinal fluid distribution in idiopathic normal pressure hydrocephalus. J. Neuroimaging 29, 242–251. https://doi.org/10.1111/jon.12581.

Zaaroor, M., Bleich, N., Chistyakov, A., Pratt, H., Feinsod, M., 1997. Motor evoked potentials in the preoperative and postoperative assessment of normal pressure hydrocephalus. J. Neurol. Neurosurg. Psychiatry 62, 517–521. https://doi.org/10.1136/jnnp.62.5.517.

Zeighami, Y., Ulla, M., Iturria-Medina, Y., Dadar, M., Zhang, Y., Larcher, K.M.-H., Fonov, V., Evans, A.C., Collins, D.L., Dagher, A., 2015. Network structure of brain atrophy in de novo Parkinson's disease. eLife 4, e08440. https://doi.org/10.7554/eLife.08440.

Zhang, H., Schneider, T., Wheeler-Kingshott, C.A., Alexander, D.C., 2012. NODDI: practical in vivo neurite orientation dispersion and density imaging of the human brain. NeuroImage 61, 1000–1016. https://doi.org/10.1016/j.neuroimage.2012.03.072.

Zhuang, X., Walsh, R.R., Sreenivasan, K., Yang, Z., Mishra, V., Cordes, D., 2018. Incorporating spatial constraint in co-activation pattern analysis to explore the dynamics of resting-state networks: an application to Parkinson's disease. NeuroImage 172, 64–84. https://doi.org/10.1016/j.neuroimage.2018.01.019.